University of Piemonte Orientale
"Amedeo Avogadro"

PhD School of Molecular Medicine

Final report

CARCINOGENESIS AND PHARMACOLOGICAL THERAPY OF MALIGNANT MESOTHELIOMA

PhD Student: Pietro Bertino
Tutor: Prof G. Gaudino

INTRODUCTION

Malignant Mesothelioma (MM) is a malignancy of the mesothelial cells that form the serosal membranes covering chest and abdominal cavities. Median survival for this cancer is about 12-18 months, and MM causes 2,000-3,000 deaths per year in the USA and about 1,000 deaths in the U.K. [1].

Asbestos refers to a group of naturally occurring hydrated mineral silicate fibers, associated to the development of pulmonary and pleural diseases. In particular, asbestos is the main cause of human MM. The various types of asbestos are divided into two major groups: serpentine, represented by chrysotile; and amphibole, which includes crocidolite, amosite, anthophyllite, actinolite, and tremolite. Crocidolite is often considered the most oncogenic type of asbestos in the causation of MM [2-4].

Only a fraction (about 5%) of subjects exposed to high levels of asbestos develop MM. This finding suggests that additional factors, such as Simian Virus 40 (SV40) infection, exposure to radiations and genetic predisposition, may render some individual more susceptible to develop MM [5].

SV40 is a monkey DNA virus that induces MM in hamsters [6]. Following this observation, numerous laboratories have detected SV40 in MM biopsies, although the prevalence of SV40 varied in different studies from about 6% to 60%, and some studies did not detect SV40 [7-9]. SV40 contaminated human polio vaccine worldwide from 1955 until 1961. Epidemiological studies comparing cohorts born before or after 1961, detected an increased relative risk of 3 for MM in pre-1961 cohorts that included many individuals vaccinated with contaminated polio vaccines [10]. Recent data supported these concerns, showing that polio vaccines prepared in Eastern Europe and distributed in many countries contained infectious SV40 at least until 1978 [11].

MM in western world is a relatively rare cancer, often associated with asbestos exposure. In contrast, among people born in Cappadocia (Turkey) villages of Tuzkoy, Karain and “Old” Sarihidir, about 50% of deaths are caused by MM. This

epidemic has been linked to erionite exposure [2, 4, 12, 13]. Erionite is a fibrous zeolite mineral formed by alteration of volcanic rocks, such as those found in the Cappadocian region of Turkey and in other geological similar areas of the world [5]. It has been shown that even very limited exposure to Cappadocian erionite fibers is sufficient to cause MM in humans and animal experiment have shown that erionite is more potent than crocidolite in causing MM [14].

It was previously reported that MM in the villages of Tuzkoy and Karain occurs predominantly in certain families, whereas families living in nearby houses do not develop MM [2, 15]. Moreover, nearby villages, such as Karlik, 1.5 Km from Karain, do not experience excess MM. These differences have been attributed to the presence of a putatively “different” type of erionite in certain houses [2]. The hypothesis that a more oncogenic type of erionite caused the MM epidemic in certain villages but not in the others seemed supported by the observation that erionite is present in California, Nevada, Oregon, etc., as well as in several European countries. However, outside Cappadocia erionite has not been linked to MM [2].

A recent study proposed a new hypothesis indicating that the MM epidemic in Cappadocian villages is caused by the interaction among the chemical carcinogen erionite with genetics. For the first time, the crystal structure and chemical composition of erionite from the Cappadocian MM villages were determined and the results were compared with the erionite from nearby non-MM villages and Oregon. This study showed that Karain, “Old” Sarihidir, the non-MM village and Roma (Oregon) have the same mineralogical kind of erionite. Moreover, within the same village, no differences in composition or in presence of erionite were found among houses with high and low or no incidence of MM; all the houses tested contained erionite [5].

My PhD program was totally dedicated to projects on MM. During the first three years, I worked in the laboratory of Prof. G. Gaudino at Department of Medical Sciences and at Department of Chemical, Food, Pharmaceutical and Pharmacological Sciences (DiSCAFF) in Novara. Prof. G. Gaudino developed a

new model for viral-related carcinogenesis of human MM where SV40 induces an HGF/Met autocrine loop in mesothelial cells [16]. Activation of tyrosine kinase receptors by ligands induces phosphatidylinositol-3 kinase (PI3K) and Akt activities, exerting several biological effects, including increased cell survival with relevant effects on MM carcinogenesis.

The aim of my research project was to elucidate the carcinogenic mechanism by which erionite causes transformation of mesothelial cells. Differently to asbestos, erionite has low cytotoxicity that allows mesothelial cells to proliferate in absence of anti-apoptotic signals. In addition, the genotoxic properties of erionite induce DNA mutations, which are fixed in proliferating cells, which are induced to transform. My contribution to this study led to a publication, as fist author, showing that erionite and asbestos differently cause transformation of mesothelial cells [17].

Carcinogenesis processes that bring to development of MM are an important issue and the knowledge of risk factors, such as SV40, mineral fibers or genetic predisposition, can help in the improvement of preventive measures to limit exposure to these risk factors and to decrease the incidence of this deadly cancer. Unfortunately, MM develops after a long latency after exposure and its incidence is expected to rise dramatically in the next years. Hence, there is urgency to develop new therapies to improve the clinical course of this disease.

My interest mostly focused on MM therapy. In particular, during my PhD program, I conducted *in vitro* and *in vivo* studies regarding the therapeutic combinations of imatinib mesylate with gemcitabine or pemetrexed. Imatinib mesylate (Gleevec®) is a tyrosine kinase inhibitor with antineoplastic activity. Imatinib binds to an intracellular pocket located within some specific tyrosine kinases, namely Bcr-Abl, Platelet-Derived Growth Factor Receptor (PDGFR), c-fms and Kit. Thereby it inhibits ATP binding and prevents tyrosine auto-phosphorylation of growth factor receptors and subsequent activation of their downstream signal transduction pathways. [18-20].

A number of chemotherapeutic agents have shown promising, as single agents or in combination with other drugs in the treatment of MM. Gemcitabine, a pyrimidine nucleoside anti-metabolite, is known to be active in patients with MM both a single agent and in combination with cisplatin. As a prodrug, gemcitabine requires intracellular phosphorylation to the active gemcitabine-nucleotides for activation. Both gemcitabine diphosphate (dFdCDP) and gemcitabine triphosphate (dFdCTP) contribute to inhibition of DNA synthesis and thereby determine antitumor activity. Gemcitabine diphosphate effectively inhibits ribonucleotide reductase inducing a depletion of cellular deoxynucleotides (dNTP) blocking DNA synthesis. On the other hand, dNTP depletion stimulates gemcitabine phosphorylation and enhances incorporation of gemcitabine nucleotides into DNA. Gemcitabine further acts as an effective inhibitor of DNA repair, as demonstrated in case of DNA damage induced by radiation or alkylating agents. Its potential as a repair inhibitor and its comparatively low toxicity profile make gemcitabine a promising agent for combination treatments [21, 22].

Pemetrexed, a multitargeted antifolate, was the first agent approved for the treatment of advanced pleural MM. Pemetrexed inhibits dihydrofolate reductase, thymidylate synthase and glycinamide ribonucleotide formyltransferase, enzymes involved in purine and pyrimidine synthesis. Pemetrexed enters the cell primarily through the reduced folate carrier, and undergoes extensive intracellular poly-glutamation by folylpoly-gamma-glutammate synthetase. In a pivotal phase III trial, the combination of pemetrexed plus cisplatin provided patients with significantly improved survival when compared with cisplatin alone. These results led to the licensing of this combination for the treatment of MM in several countries [22, 23].

I started my work in Gaudino's lab while the effects of the combination imatinib mesylate-gemcitabine on MM cells were just discovered. Gaudino and his collaborators exploited the method known as "Isobologram", where an algorithm allows to assess whether a drug combination dose is additive, subadditive or

superadditive (synergistic) [24]. In the “Isobologram” a particular “effect” level is selected. For example, in our studies we utilized the lethal drug dose that kills 50% of cells (LC_{50}). Generating dose-response curves, we started calculating LC_{50} for each drug. Consecutively, we plotted LC_{50}s of drug A (e.g. gemcitabine) and drug B (e.g. imatinib mesylate) as different axial points in a Cartesian plot. The straight line connecting both LC_{50}s is the locus of points (dose pairs) in which 50% of cells are killed in the case of a simply additive combination. This line of “additivity” allows a comparison with LC_{50}s produced experimentally by the tested dose pair. At this purpose, we generate a series of dose-response curves for drug A in the presence of several fixed concentrations of drug B. The resulting LC_{50}s are plotted in the isobologram. If the experimental LC_{50}s appear below of the additive line, it means that experimental dose pair produces the same effect with lesser quantities and are superadditive (synergistic). On the other hand, if the experimental LC_{50}s are above the additive line, it means that greater quantities of drugs in combination are required to give the same effect of the sum of drugs alone and are therefore subadditive.

By using the “Isobologram” method, we revealed that imatinib mesylate also synergistically enhances effects of pemetrexed. Moreover, we described that the enhancement of tumor chemosensitivity by imatinib mesylate was proportional to the number of receptors responsive to this drug in MM cells. These results together allowed us to propose a novel translational approach to MM treatment [25].

The next step in this project was to evaluate the effects of the imatinib-combined therapy combinations in a suitable animal model. By injecting MM cells in the peritoneum of SCID mouse we established a MM mouse xenogeneic model. This is an excellent model for therapeutic studies because the tumor develops producing numerous nodules that cover the peritoneal cavity, similarly to what happen in humans, where MM produces numerous nodules that cover the pleural cavity. However, numerous nodules were difficult to measure and, at this purpose, we developed a most appropriate method to measure tumor

dimensions changes over time. We genetically engineered MM cells, by lentiviral expression of recombinant *luciferase,* which allows photon emission in the presence of the luminol substrate. By injection of these cells into the peritoneal cavity of SCID mice, we developed a MM mouse model in which tumor measurement could be done by IVIS imaging system (Xenogen Corp.). Among several cell lines tested, REN mesothelioma cells successfully grew in SCID mice, although they are more resistant to pemetrexed than to gemcitabine. By using this model we assessed *in vivo* the synergism of imatinib mesylate with gemcitabine, but not with pemetrexed [26]. These results confirmed the *in vitro* data previously published and allowed us to design a phase II clinical trial currently ongoing. Further studies with different luminescent cells should be conducted to ascertain the real effectiveness of a combined treatment of imatinib mesylate with pemetrexed.

In the last year of my PhD program, Gaudino's group established a collaboration with Prof. M. Carbone of the University of Hawaii. Prof. Carbone has been the first to study effects of SV40 in hamsters and to discover human poliovirus vaccines contaminated by SV40 [6, 11]. Moreover, he conducted the investigations previously mentioned to elucidate the role of genetics in MM epidemic in Cappadocian villages. Our experience on erionite carcinogenesis *in vitro* is the basis for the collaborative effort with Dr. Carbone to establish the effect of these finres *in vivo*. At this purpose and to complete the stage requested by my PhD school, I joined the laboratory of Prof. Carbone in June 2007.

Int. J. Cancer: **121,** 12–20 (2007)

Erionite and asbestos differently cause transformation of human mesothelial cells

P. Bertino[1], A. Marconi[2], L. Palumbo[2], B. M. Bruni[2], D. Barbone[1], S. Germano[1], A.U. Dogan[3,4], G. F. Tassi[5], C. Porta[6], L. Mutti[7] and G. Gaudino[1]*

[1]*Department of DISCAFF and DFB Center, University of Piemonte Orientale ''A. Avogadro'', Novara, Italy*
[2]*Department of Environment and Primary Prevention, Department of Technology and Health, ISS, Roma, Italy*
[3]*Department of Geological Engineering, Ankara University, Turkey*
[4]*Department of Chemical and Biochemical Engineering, University of Iowa, Iowa City, IA, USA*
[5]*Chest Medicine Unit, Brescia Hospital, Brescia, Italy*
[6]*Medical Oncology, IRCCS San Matteo University Hospital, Pavia, Italy*
[7]*Local Health Unit, 11 Piemonte, Italy*

Malignant mesothelioma (MM) is an aggressive tumor associated with environmental or occupational exposure to asbestos fibers. Erionite is a fibrous zeolite, morphologically similar to asbestos and it is assumed to be even more carcinogenic. Onset and progression of MM has been suggested as the result of the cooperation between asbestos and other cofactors, such as SV40 virus infection. Nevertheless, several cases of MM were associated with environmental exposure to erionite in Turkey, where SV40 was never isolated in MM specimens. We show here that erionite is poorly cytotoxic, induces proliferating signals and high growth rate in human mesothelial cells (HMC). Long term exposure to erionite, but not to asbestos fibers, transforms HMC *in vitro*, regardless of the presence of SV40 sequences, leading to foci formation in cultured monolayers. Cells derived from foci display constitutive activation of Akt, NF-κB and Erk1/2, show prolonged survival and a deregulated cell cycle, involving cyclin D1 and E overexpression. Our results reveal that erionite is able *per se* to turn HMC into transformed highly proliferating cells and disclose the carcinogenic properties of erionite, prompting for a careful evaluation of environmental exposure to these fibers. The genetic predisposition to the effect of erionite is a separate subject for investigation.
© *2007 Wiley-Liss, Inc.*

Key words: asbestos; zeolite; erionite; mesothelioma; cell transformation

Environmental or occupational exposure to asbestos fibers may cause chronic respiratory diseases, including interstitial lung fibrosis and pleural malignant mesothelioma (MM).[1,2] Pedigree and mineralogical studies indicate that the high incidence of MM in a number of Cappadocia villages in Turkey is caused, in genetically predisposed individuals, by exposure to fibrous erionite. This is a highly pathogenic form of the naturally occurring zeolite, similar in appearance and properties to asbestos.[3,4] Erionite is a strong mutagen,[5] considered more carcinogenic than asbestos fibers in man and rodents,[6] possibly due to the peculiar property of accumulating iron on its surface, despite its very small content of this element.[7] It is well documented that erionite from Oregon has genotoxic properties[8] and induces high incidence of MM in rats after both intrapleural inoculation or inhalation,[9] although there are no epidemiological data correlating the presence of erionite to MM in Oregon.

Similarly to what occurs with asbestos, exposure to erionite fibers leads to generation of reactive oxygen metabolites from macrophages[10] and to increased mRNA levels of the early response c-fos and c-jun proto-oncogenes in mesothelial cells.[11,12] MAPK signaling significantly contributes to pivotal cell functions as cell proliferation and death in response to toxic and inflammatory agents.[13] Similarly, PI3K/Akt and NF-κB signaling play a crucial role in determining cell fate after exposure to toxic agents[14,15] and are activated by asbestos fibers as well.[16,17] Interestingly, TNF-α inhibits asbestos-induced cytotoxicity *via* a NF-κB-dependent pathway.[18] These results underscore the key role played by NF-κB in asbestos-induced oncogenesis of human mesothelial cells (HMC). Epidermal growth factor receptor (EGFR) overexpression and activation have been linked to asbestos-induced proliferation.[19] Autocrine loops for both EGFR and platelet derived growth factor receptor (PDGFR) have been also reported in MM cells.[20] Moreover, we previously demonstrated that an autocrine circuit involving hepatocyte growth factor (HGF) and its receptor Met contributes to HMC transformation[21] and others showed that Met is overexpressed in MM cells.[22]

In vitro studies demonstrated that SV40 and asbestos fibers cooperate to determine HMC transformation,[23] *via* PI3K/Akt signaling.[24] Therefore, here we compared the proliferating and transforming efficacy of short- and long-term exposures of HMC to erionite, amosite, chrysotile or glass fibers, in absence of SV40 infection. Moreover, to achieve a better understanding on the mechanism by which these fibers determine cell transformation, we further evaluated tyrosine kinase receptor expression and signal transduction in HMC transformed by the different fibers.

Our data reveal that erionite fibers have higher intrinsic transformation ability than asbestos fibers and give a possible explanation for the high incidence of MM in 3 small villages in Turkey, where SV40 virus infection of MM cells has never been detected.[3,4,25,26]

Material and methods

Fibers

The sample of erionite fibers from Karain, provided by co-author Dr. Umran Dogan (Ankara, Turkey), was associated with considerable amounts of nonfibrous particles and bundles, with diameter greater than 3 μm and length-to-width ratio (L/W) less than 3:1. The fraction of fibrous material with L/W of 3:1 or greater in this sample is less than 10% by weight, because erionite in Karain occurs as a minor constituent of a volcanic amorphous rock, from which the erionite mineral originates.[4,9,27–29] The erionite sample from Oregon, kindly provided by Dr. J. W. Skidmore (Glamorgan, UK), was almost totally made of fibrous particles.

No milling, crushing or ultrasound processing was performed prior to size analysis. Representative portions of each erionite sample was weighted (5 ± 0.5 mg) and dispersed in 20 ml of filtered, deionized, distilled water. About 0.45 ml of the dispersion

Grant sponsors: AIRC (Associazione Italiana per la Ricerca sul Cancro), MARF (Mesothelioma Applied Research Foundation), Buzzi Unicem Foundation for mesothelioma research.
The last two authors equally contributed to this work.
***Correspondence to:** Giovanni Gaudino. DISCAFF Department, University of Piemonte Orientale ''A. Avogadro'', via Bovio, 6, Novara 28100, Italy. Fax: +39-0321-375821.
E-mail: giovanni.gaudino@unipmn.it
Received 8 June 2006; Accepted after revision 2 February 2007
DOI 10.1002/ijc.22687
Published online 12 March 2007 in Wiley InterScience (www.interscience.wiley.com).

was filtered on a policarbonate filter (0.1 μm), dried, placed on aluminum stub and plated with gold in a sputter coater.

Each sample was examined using a Philips XL30 scanning electron microscope (SEM) at different magnifications, to determine dispersion and visibility of the fibers. Central fields with adequate fibers dispersion were selected for each sample and length (L) and width (W) of fibers were measured directly on the SEM screen with the ruler of the microscope. Fiber bundles with L/W of 3:1 or greater were considered as single fibers. L and W measurements of about 500 fibers were recorded for each fibrous sample. The size analysis of glass fibers was similarly performed.

Size distribution of UICC asbestos samples (Chrysotile B and Amosite) were acquired from previous data obtained by transmission electron microscopy.[30]

Erionite (Karain-Turkey and Oregon-USA), amosite, chrysotile (UICC asbestos samples) and glass fibers were dispersed in PBS at 2.0 mg/ml, before autoclaving. Then, amosite, chrysotile and glass fibers, but not erionite fibers, were triturated 8 times through a 22-gauge needle.

Cell cultures

Two primary HMC cell cultures, obtained from patients with heart failure were cultured in Ham's F-12 medium, supplemented with 10% fetal bovine serum (FBS–GIBCO, Rockville, MD) at 37°C in a 5% CO_2-humidified atmosphere. HMC were used between the second and the sixth passage. Both cultures gave similar results in all assays performed, as previously characterized.[24]

DNA-neosynthesis

HMC cells were exposed to medium containing 2% FBS supplemented with fibers in presence of 10 μM BrdU (Bromo-deoxy-Uridine). Incorporation in neosynthesized DNA was evaluated after 24 hr by the cell proliferation kit (Roche, Basel, Switzerland). Data are expressed as mean increase of DNA-neosynthesis over untreated controls.

Cytotoxicity and DNA *adducts*

Cells were seeded on multiwell plates and 5×10^3 cell/well were exposed for 24 or 48 hr to fibers at densities ranging from 2 to 10 μg/cm^2 in presence of 2% FBS. Experiments performed on foci derived cells were conducted in presence of 100 μM VP16 (Etoposide, Sigma-Aldrich, St. Louis, MO), for 24 hr. Cytotoxicity was assessed by MTT assay, performed in quadruplicate, as previously described.[31] Normalized cytotoxicity percentages were obtained according to the ratio: [1-(A_{570} mean values of extracts from exposed samples/A_{570} mean values of extracts from control cell samples)] × 100.

DNA adducts were evaluated by high-performance liquid chromatography (HPLC), in the presence or absence of 10 mM *N*-Acetyl-L-cysteine (L-NAC) (Sigma-Aldrich, St. Louis, MO), on extracts from cells exposed for 5 hr at 10 μg/cm^2 to the indicated fibers and are expressed as amount of 8-OHdG per 10^5 dG, as previously described.[32]

Exposure to fibers

Short term exposure. Stimulation of sub-confluent cells for 24 hr with medium containing 20% FBS supplemented with fibers at concentrations ranging from 0.1 to 10 μg/cm^2.

Long term exposure. Two cycles of treatment, 72 hr each, with low concentrations of fibers. In details, 1 day after plating at 80% confluence in 25 ml flasks, cells were exposed to 2.5 μg/cm^2 of each fiber for 72 hr. Then, cells were washed twice with PBS and cells were transferred in larger (75-and 150-cm^2) flasks and let growing in medium containing 10% FBS for additional 4 days. Afterwards, the same fiber treatment was repeated as above and cells were grown up to 2 months, by 1:4 periodical passages. Treatments were made in triplicate.

Apoptosis

Sub-confluent cells were exposed to Ham's medium supplemented with 2% FBS, containing fibers (10 μg/cm^2) or 100 μM VP16 (Etoposide, Sigma-Aldrich, St. Louis, MO) for 24 hr. Nuclei fragmentation was evaluated by staining cells grown on cover slips with 8 μg/ml Hoechst solution (Calbiochem, San Diego, CA) in dark conditions for 1 hr. Samples were fixed in –20°C cold acetone:methanol for 15 min, washed in PBS, mounted in 50% glycerol/PBS and observed with a Leica immunofluorescence microscope. Cells displaying nuclear fragmentation were counted on 10 fields out of at least 50 cells in the same slide. Values are expressed as percentages of Hoechst staining positive HMC over total counted cells. Caspase activity was evaluated by staining cells with CaspACE FITC-VAD-FMK *in situ* marker (Promega, Madison, WI), followed by flow cytometry.

Signal transduction

Immunoblotting was performed by loading 50 μg of cell lysates in reducing conditions. After separation on SDS-PAGE and transfer to nitrocellulose (Hybond, Amersham, Buckinghamshire, UK), filters were probed with phospho-p38 (Thr180-Tyr182), phospho-NF-κB p65 (Ser536), phospho-JNK (Thr183-Tyr185), phospho-Akt (Ser473), phospho-Erk1/2 (Thr202-Tyr204), Akt, Erk1/2 antibodies from Cell Signalling Technology, Beverly, MA, α-Tubulin antibodies from Sigma-Aldrich as loading controls, Met, EGFR, PDGFRβ, NF-κB p65, JNK, p38, Cyclin D1 and E antibodies from Santa Cruz Biotechnology, Santa Cruz, CA. Detection was performed by the enhanced chemiluminescence system (ECL, Amersham).

Focus forming assay

Cells that survived the ''long term'' exposure to fibers, were followed 8 weeks, then a focus forming assay was performed in triplicate in 6-well dishes. Cells were plated at a density of 3×10^4/well and grown in 10% FBS Ham's medium. The number of foci per number of seeded cells is expressed as mean number ± standard deviation (SD). Foci arisen from confluent cells were taken and successfully established in cultures as single clones. Biochemical and biological characterization of foci were performed on a pool of clones, with a representative mixture of cells from each original focus.

Cell proliferation

Cells were grown on 24-well plates at a density of 3×10^4/well in Ham's medium supplemented with 2% FBS and containing the indicated fibers (1.25 μg/cm^2). Cells were fixed in 11% glutaraldehyde after 0, 24, 48 and 72 hr exposure and stained in crystal violet staining was eluted in 10% acetic acid and absorbance at 595 nm (A595) was measured in an ELISA plate reader.[33]

Immunochemical staining

Sub-confluent cells plated on glass slide flaskets (NUNC, Rochester, NY) were exposed to Ham's medium supplemented with 2% FBS and containing fibers (10 μg/cm^2) for 24 hr and subsequently fixed in 10% formalin. After 1 hr incubation with Ki67 antibodies (Neomarkers, Freemont, CA) at room temperature, biotin-streptavidin immunostaining was performed with UltraVision detection system, according to the manufacturer's instructions. Ki67 positive cells were counted on 10 fields with at least 50 cells in the same slide. Values are expressed as percentages of Ki67 positive cells over total counted HMC.

Cell cycle

Cells were synchronized by 0.1 μg/ml Colcemyd (Sigma-Aldrich) treatment for 24 hr, and then kept in normal medium for 4 days before analysis. They were washed in PBS, fixed in 50% ethanol and stained for 30 min at room temperature with 50 μg/ml propidium iodide (PI-Sigma-Aldrich) in 0.1 M PBS pH 7.2

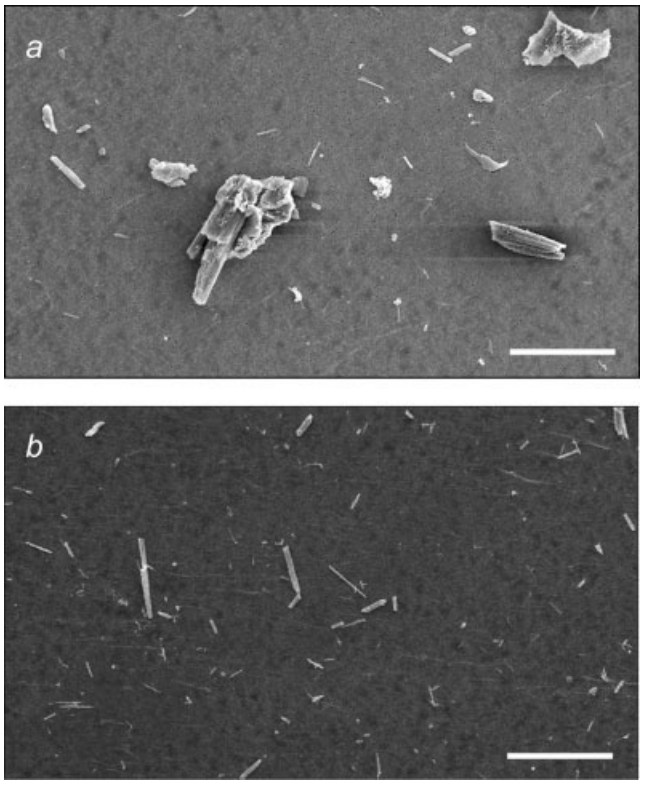

FIGURE 1 – SEM analysis of erionite fiber samples. SEM analysis of Karain (*a*) and Oregon (*b*) fiber samples at ×500 magnification. Central fields with adequate dispersion of fibers were selected for each sample. Bar: 50 μm.

containing 0.5 mg/ml RNAse. 10,000 events per sample were analyzed by flow cytometry.

Statistics

Data from cytotoxicity, DNA adducts, cell cycle, DNA neosynthesis, proliferation assays and caspase activity were expressed as mean ± standard deviation (SD) of at least 3 independent experiments. Statistical differences were evaluated by analysis of variance (ANOVA), followed by Tukey's HSD. Statistical analysis of Ki67 immunostaining and Hoechst staining assays was performed by Fisher's exact test among different groups, as indicated in the text. In all statistical evaluation the significance threshold was specified in the text. All statistical tests were two-sided.

Results

Most of erionite fiber samples fall in a mineralogical category with lower cytotoxicity than asbestos fibers

Karain erionite is a minor constituent of a volcanic rock, which is mainly Si-rich glass.[4,9,27–29] In addition, montmorillonite, and traces of quartz, feldspar, opal, clay (illite), carbonates were found associated with rock and soil samples from Karain.[27,28] For these reasons, the preparation of an adequately fiber-enriched sample for our tests was not possible. Nevertheless, in accordance with previous studies,[28] most of the matrix particulate material associated to the erionite used here is amorphous glass and few clay, carbonate and feldspar minerals. The erionite sample was characterized as having acceptable balance error, to verify that the data obtained fit with chemical composition and structure of the tested mineral.

TABLE I – NUMBER OF FIBRES IN DIFFERENT DIMENSIONAL CATEGORIES BY SEM

Fibre diameter (μm)	Fibre length, μm (%)		
	≤5	>5–8	>8
Oregon erionite (n = 495)			
>1.5	1 (0.2)	3 (0.6)	41 (8.2)
>0.5–1.5	36 (7.2)	55 (11.1)	69 (14.0)[1]
≤0.5	117 (23.6)	94 (19.0)	79 (16.1)[1]
Karain erionite (n = 500)			
>1.5	1 (0.2)	8 (1.6)	82 (16.4)
>0.5–1.5	38 (7.6)	69 (13.8)	97 (19.4)[1]
≤0.5	87 (17.4)	85 (17.0)	33 (6.6)[1]

[1]Proportion of fibres falling into the dimensional category with highest neoplastic response.

TABLE II – SIZE DISTRIBUTION (%) OF UICC ASBESTOS SAMPLES[23]

UICC sample	$L \geq 8$ μm	$D \leq 1.5$ μm
Chrysotile B	88	100
Amosite	70	99

From SEM examination the fraction of Karain fibrous material with L/W of 3:1 or greater resulted to be in the range 5–10%. In the erionite sample from Oregon this fraction resulted about 75%, with nonfibrous particles being mostly of amorphous nature (Fig. 1), in accordance with previous studies.[34]

The distribution of fiber sizes of the erionite samples are shown in the Table I. The fraction of fibers ($L > 8$ μm and $W \leq 1.5$ μm) with the dimensional category suggested as having the highest carcinogenic potential in rats ($L > 8$ μm and $W \leq 1.5$ μm)[35] was 26.0 and 30.1% in the Karain and Oregon samples, respectively. As shown in Table II, the size distribution of UICC asbestos samples (chrysotile B and amosite) reveals that all particles were asbestiform fibers with diameters smaller than 1 μm. However, the fraction of fibers with $L > 8$ μm was 88 and 70% for chrysotile and amosite, respectively.

Calculations made on the basis of size distributions of Karain and Oregon erionite fibers revealed that the dust in size range considered more biologically active was constituted of ~19 and 180 fibers per microgram (F/μg) respectively, whereas the UICC chrysotile sample had about 1.5×10^5 and UICC amosite 1.2×10^5 F/μg. Noteworthy, the number of Oregon erionite fibers expressed in F/μg was very close to the value (150 F/μg) previously reported.[8]

Therefore, the fraction of more biologically active fibers was considerably lower in the case of erionite fibers, as compared to UICC asbestos samples, particularly in the case of erionite from Karain. In the glass fiber sample only a very small percentage (about 1%) of fibers were included in the more pathogenic size range.

Erionite induces low cell death but high DNA *neosynthesis*

We compared cytotoxicity induced by Karain (Turkey) and Oregon (USA) erionite fibers with that of asbestos fibers (amosite and chrysotile) and of glass fibers, used as relatively inert control. HMC were exposed for short term (24 hr) to fiber suspensions ranging from 0.1 up to 10 μg/cm^2, and cytotoxicity was evaluated by MTT assay. Our data show that dose-dependent cytotoxicity occurred in HMC exposed to erionite fibers, although by far lower than that induced by amosite. The differences evaluated at 5 and 10 μg/cm^2 at 24 hr are statistically significant ($p \leq 0.001$). Conversely, chrysotile-induced cytotoxicity was comparable with that of erionite. As expected, no detectable cytotoxicity was induced by glass fibers. After 48 hr the cytotoxic response was uniformly increased and differences among amosite and erionite fibers in

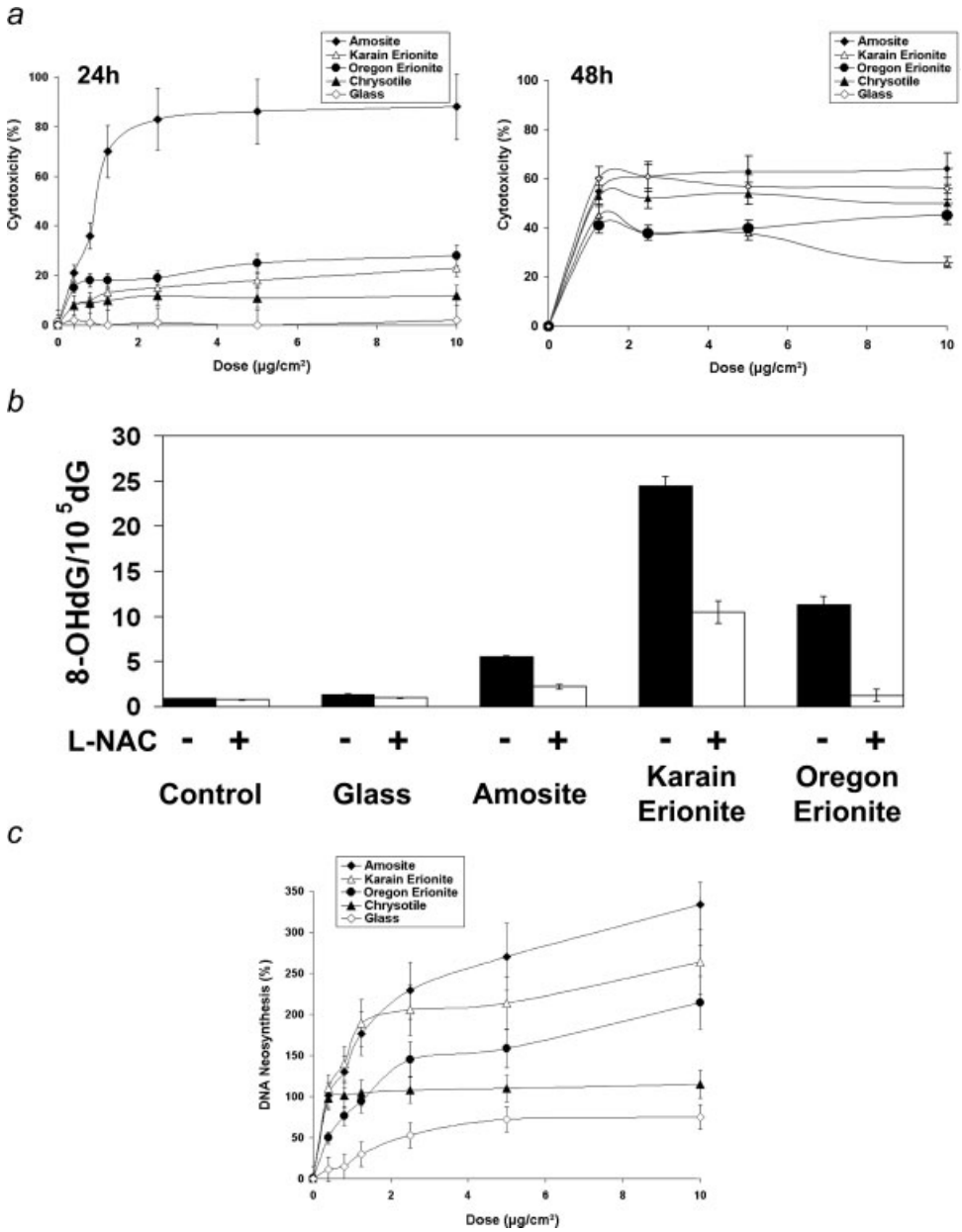

FIGURE 2 – Short term exposure to erionite and asbestos induces cytotoxicity, DNA adducts and DNA neosynthesis. (*a*) Cytotoxicity evaluated by MTT assay at different doses of the indicated fiber types, after short term exposure of 24 and 48 hr. (*b*) DNA content of 8-OHdG in HMC exposed to the indicated fibers, in presence or absence of L-NAC, evaluated as number of adducts formed per 10^5 dG. (*c*) BrdU incorporation in neosynthesized DNA of HMC cells, after 24 hr exposure to different doses of the indicated fiber types, expressed as percentage over untreated control.

inducing cell death were less evident, albeit erionite fibers at 5 µg/cm^2 still significantly displayed lower cytotoxicity levels than amosite ($p \leq 0.005$) and even than glass ($p \leq 0.05$) (Fig. 2*a*). These results were confirmed when apoptosis was evaluated by counting apoptotic cells after Hoechst staining. A higher number of nuclei showing typical chromatin condensation was observed upon cell exposure to pro-apoptotic agent VP16 (11.3%) and to amosite (12.4%), than in cells exposed to Karain erionite (3.9%), Oregon erionite (5.6%) or to glass beads (2.5%). These differences were statistically significant ($p \leq 0.001$). The possible effects of oxidative stress by fibers were examined by 8-hydroxy-2′-deoxyguanosine (8-OHdG) evaluation with HPLC and UV/amperometric detection. Interestingly, amosite and erionite fibers significantly induced DNA damage as compared to unexposed controls or to glass ($p \leq 0.001$). However, the amount of adducts induced by both erionite fibers was by far higher than that induced by amosite ($p \leq 0.001$). When the exposure to fibers was conducted in presence of the anti-oxidant agent *N*-Acetyl-L-Cysteine (L-NAC), the amount of DNA adducts significantly decreased for amosite and erionite fibers ($p \leq 0.001$), (Fig. 2*b*). This strongly indicates that oxygen reactive species play a role in DNA damage induced by exposure to fibers. Moreover, cell exposure to amosite or erionite fibers at 10 µg/cm^2 induced significantly higher BrdU incorporation in comparison with exposure to glass beads ($p \leq 0.005$) or chrysotile ($p \leq 0.05$), (Fig. 2*c*).

Only erionite-induced DNA *neosynthesis leads to cell proliferation*

Cell proliferation was monitored in HMC cultures to verify whether the considerable DNA neosynthesis observed upon erionite exposure was due either to compensatory synthesis of DNA, to repair fiber-induced chromosome damage, or to actual cell proliferation.

We observed an evident, although not statistically significant, increase in cell proliferation rate after 24 hr upon exposure to both types of erionite fibers, as compared to amosite, chrysotile and

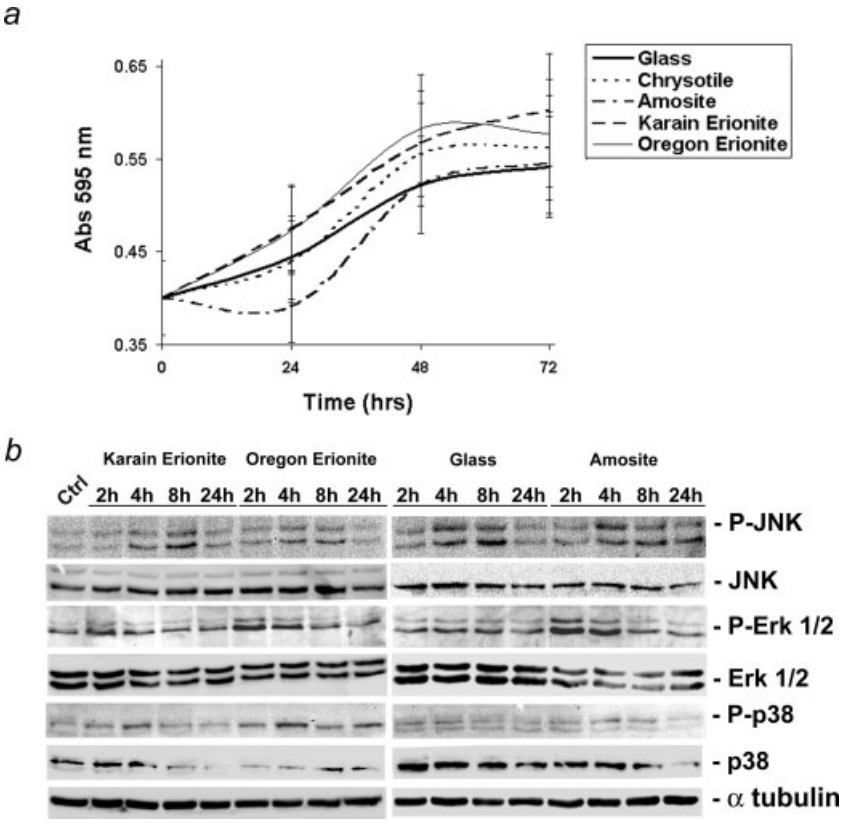

FIGURE 3 – Erionite-induced DNA neosynthesis is not only compensation for DNA damage. (*a*) Cell growth curve of HMC exposed to the indicated fibers and monitored at 24, 48 and 72 hr. Cell number was estimated by Abs595 nm values of the adsorbed crystal violet. (*b*) Immunoblotting with phospho-JNK, phospho-ERK1/2 and phospho-p38 antibodies on total lysates of HMC exposed to the indicated fibers for 2, 4, 8 and 24 hr. The expression levels of JNK, ERK1/2 and p38 were also examined by immunoblotting and α-tubulin content is also reported as loading control.

glass fibers exposure. After 72 hr, these differences were still evident, even though cells were sub-confluent and attained the growth plateau (Fig. 3*a*). Also Ki67 staining, a known cell proliferation marker, was determined upon 24 hr exposure to amosite, glass and both types of erionite fibers. Higher percentages of Ki67-positive cells were found in HMC cultures exposed to Karain erionite (6.2%) and to Oregon erionite (5.0%), as compared to amosite (2.6%) or glass (2.1%) fibers, as well as to untreated cells (3.2%). The differences in Ki67 staining induced by both erionite fibers compared to other fiber types are statistically significant ($p \leq 0.005$). Moreover, transient Jnk phosphorylation was observed 4 hr after exposure to any fiber type (10 μg/cm^2), suggesting a nonspecific stress response (Fig. 3*b*). Jnk phosphorylation decreased after 8 hr, except in the case of amosite, which evoked instead a sustained Jnk activity, as expected from its high level of cytotoxicity. Erk1/2 and p38 phosphorylation was not detectable after exposure to glass fibers, whereas Erk1/2 phosphorylation was sustained up to 8 hr after exposure to amosite. In cells exposed to erionite fibers Erk1/2 signaling was more transient. The activity of p38 was by far more evident in cells exposed to erionite than amosite, especially in consideration of a reduced p38 expression in erionite treated cells (Fig. 3*b*). In cells exposed to amosite fibers we observed: reduced proliferation rate (Fig. 3*a*), increased cell death (Fig. 2*a*) and significantly lower staining of Ki67, but also elevated BrdU incorporation (Fig. 2*c*) and sustained Erk1/2 activity (Fig. 3*b*). One possible interpretation of these data is that DNA neosyntesis occur in cells nevertheless dying, as a consequence of amosite damage.

As regards erionite fibers, we conclude that DNA-neosynthesis observed after short term exposure to fibers is not only compensatory in consequence of erionite-induced DNA damage, but also allows HMC proliferation. Moreover, the exposure to erionite fibers, displaying low cytotoxicity and high production of reactive oxygen species, exerts on HMC the highest transforming potential.

TABLE III – FOCI FORMED AFTER 60 DAYS ''LONG TERM'' EXPOSURE TO DIFFERENT FIBRE TYPES

Treatment	Frequency of focus formation[1]
Untreated	–[2]
Glass	–[2]
Amosite	–[2]
Chrysotile	–[2]
Karain erionite	$1.0 \times 10^{-4} \pm 0.65 \times 10^{-4}$
Oregon erionite	$0.3 \times 10^{-4} \pm 0.46 \times 10^{-4}$

[1]Number of transformed foci per treated cell.–[2]No foci developed from 3×10^5 cells exposed to fibres.

Erionite fibers ''long-term'' exposure promotes HMC transformation per se

It has been demonstrated that prolonged exposure of SV40 positive-HMC to asbestos fibers may induce transformation.[23,24] We aimed to verify whether exposure to low doses of erionite fibers could induce mesothelial transformation and if SV40 is required, as for asbestos fibers. We treated HMC according to a ''long term'' exposure protocol (see Methods). Two months after the ''long term'' exposure, only cells exposed to erionite fibers underwent loss of cell contact inhibition and several foci arose from the culture. No statistically significant differences were observed between the 2 types of erionite fibers in focus formation. No foci resulted after exposure to amosite, chrysotile and glass fibers (Table III). These cells acquired a clear-cut novel morphology, similar to what we previously described[24] for cells exposed to asbestos (Fig. 4*a* left). Cells obtained from foci were cultured up to 29 passages for HMC-Karain erionite and 48 passages for HMC-Oregon erionite. These cells maintained the phenotype described earlier, grew in low serum, displayed anchorage-independent soft-agar growth and showed a significantly higher proliferation rate than HMC (at 48 hr, $p \leq 0.05$ for

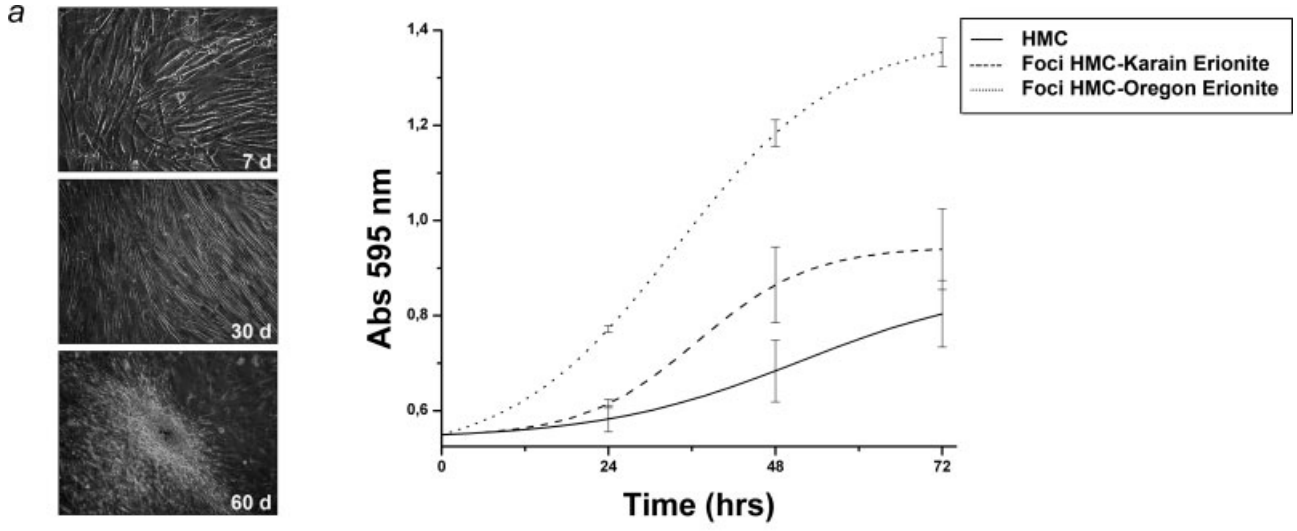

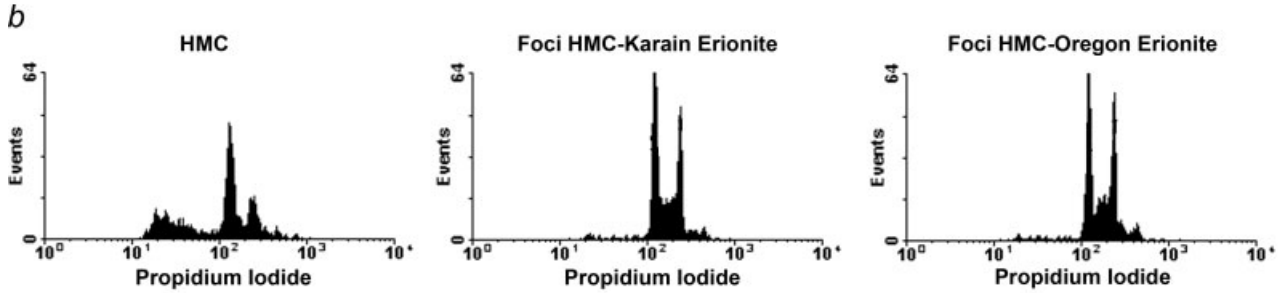

	sub-G1	G1	S	G2-M
HMC	31.81 ± 2,72	44.03 ± 3,01	6.20 ± 1,25	18.29 ± 1,43
Foci HMC-Karain Erionite	3.65 ± 1,07	49.50 ± 2,96	18.60 ± 1,51	29.73 ± 2,81
Foci HMC-Oregon Erionite	3.72 ± 0,89	51.74 ± 3,04	19.27 ± 1,61	26.88 ± 2,68

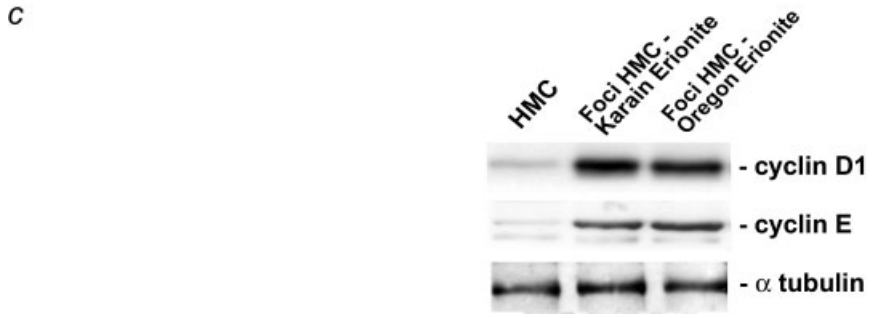

FIGURE 4 – Erionite fibers ''long-term'' exposure *per se* promotes HMC transformation. (*a*) Left: representative pictures of HMC 7, 30 and 60 days after the long-term exposure to Karain erionite fibers, showing the different acquired morphology. Right: proliferation assay of pooled cell clones from foci obtained after long term exposure to both types of erionite fibers. Cell number was estimated by Abs595 nm values of the adsorbed crystal violet. (*b*) Cell cycle analysis of synchronized HMC and cells derived from foci elicited by exposure to the two types of erionite. The percentages of cells in the different phases of the cell cycle are given in details below the cytograms. (*c*) Immunoblotting on total lysates of HMC and of foci derived cells probed with cyclin D1 and cyclin E antibodies. Same filter and loading controls of Figure 5, determined by α-tubulin immunoblotting.

HMC-Karain erionite and $p \leq 0.005$ for HMC-Oregon erionite; Fig. 4*a* right).

Cell cycle analysis revealed that cells obtained from foci, which escaped serum-dependency for growth, exhibited disappearance of subG1-S hypoploid phase, displayed a strong increase of S-phase entry (Fig. 4*b*). The differences between percentages of foci cells and HMC in subG$_1$-phase and in S-phase are statistically significant ($p \leq 0.001$). Moreover, we observed over expression of cyclins D1 and E, involved in G1/S cell cycle transition (Fig. 4*c*). In foci derived cells HGFR/Met, EGFR and PDGFRβ were expressed at higher extent than in HMC, as determined by immunoblotting. Analysis of cell signaling revealed that these cells displayed Akt, Erk1/2 and NF-κB activities at higher levels than in untransformed HMC (Fig. 5). Moreover, cells derived from foci became significantly more resistant ($p \leq 0.001$ for HMC-Karain Erionite and $p \leq 0.005$ for HMC-Oregon Erionite) than HMC to

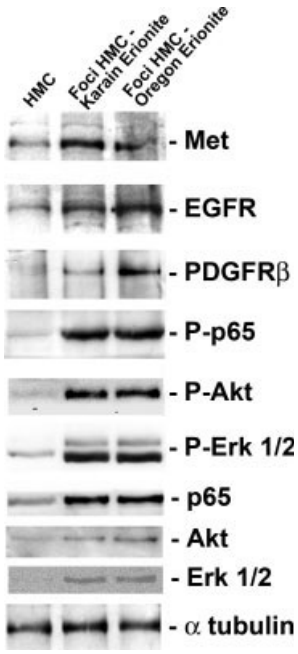

FIGURE 5 – Characterization of cells derived from foci. Immunoblotting on total lysates of HMC performed using either antibodies directed against growth factor receptors (Met/HGFR, EGFR, PDGFRβ) and phospho-specific antibodies recognizing the active form of intracellular effectors (P-p65 NF-κB, P-Akt, P-Erk1/2). Levels of p65, Akt and Erk1/2 were also determined by immunoblotting. The content of cellular proteins has been normalized by α-tubulin immunoblotting.

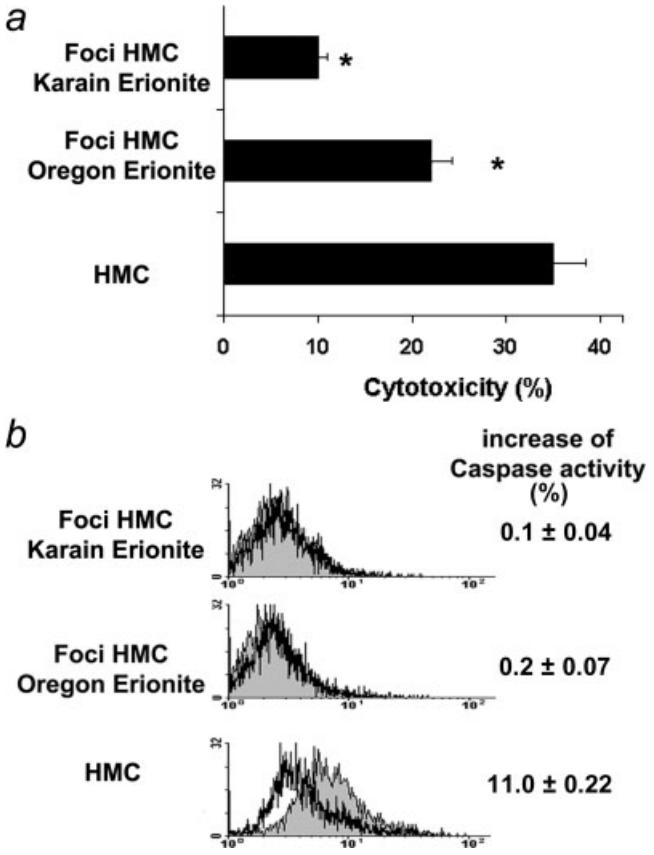

FIGURE 6 – Cells from foci become resistant to toxics. (*a*) Cytotoxicity of the indicated cell types (HMC and cells derived from foci), after exposure to 100 μM VP16, evaluated by MTT assay. (*b*) Cytofluorimetric analysis of caspase activity, by using the CaspACE FITC-VAD-FMK marker, of HMC and cells derived from foci, after exposure to 100 μM VP16. The percentage of caspase activity increase is indicated on the right.

the pro-apoptotic agent VP16 (Etoposide), as determined by MTT assay (Fig. 6*a*). As well, induction of Caspase activity, evaluated by flow cytometry, was significantly reduced in foci ($p \leq 0.001$) as compared with untransformed HMC (Fig. 6*b*).

We conclude that even relatively low concentrations of erionite fibers can cause transformation of HMC.

Discussion

Our results show that erionite has clear intrinsic transforming properties, associated with low cytotoxicity and high oxygen reactive species formation, combined with high DNA neo-synthesis and high cell proliferation rate. Cell transformation is demonstrated by foci formation in cultures exposed to erionite but not to amosite fibers. Transformed cells obtained from erionite induced foci are highly proliferating and resistant to apoptosis. HGFR/Met, EGFR and PDGFRβ are highly expressed as well, and the intracellular signalling effectors NF-κB, Akt and Erk are also activated.

The characterization by SEM analysis of the fibers used, reveals that the proportion of fibers with $L > 8$ μm and $W \leq 1.5$ μm, close to the dimensional category associated with the highest biological activity,[35] was considerably lower for erionite compared to UICC asbestos samples, very rich of fibers in the ''biologically active'' size range. The nonfibrous material present in our erionite samples should not have a substantial pathogenic influence.[36] However, we cannot exclude a possible potentiating effect by some components of this material to the action of the fibrous fraction.[37]

It has been demonstrated that the number of erionite fibers required to develop peritoneal mesothelioma in rats was orders of magnitude lower than that observed for asbestos fibers.[38] This explained the higher carcinogenic potential observed for erionite, even at considerably lower concentration than asbestos.[6]

In the present work, the comparison of asbestos with erionite fibers indicate that amosite induces relevant HMC cytotoxicity, possibly because of their longer fibers or high iron content.[39] Conversely, only erionite fibers promote HMC transformation, possibly because these fibers are less cytotoxic than amosite, having a lower content of iron.[7] Chrysotile fibers, in spite of their reduced cytotoxicity, are unable to cause cell proliferation, as previously reported.[40] Even short term exposure for 24 hr to erionite fibers induced low cytotoxicity, allowing a high proliferation rate, associated with formation of DNA adducts.

Upon fiber exposure several intracellular signals are generated. Jnk was increased by all fiber types, suggesting a nonspecific stress response and its activity was sustained only upon amosite exposure, probably because of the high cytotoxic property of these fibers. The transient patterns of Erk1/2 activity observed in HMC exposed to amosite fibers were similar to those previously reported for crocidolite exposure,[16] which has the same cytotoxicity pattern of amosite.[24] Erionite- and amosite-dependent Erk1/2 activity was consistent with cell proliferation evoked by these fibers.[12] Higher p38 activity in HMC upon exposure to erionite, can be explained with the highest oxidative stress caused by these fibers[41] and is consistent with highest levels of 8OH-dG observed here in the same conditions.

In view of the high level of BrdU incorporation in cells otherwise displaying high percentage of cell death, we interpret DNA incorporation as caused by neo-synthesis of DNA in cells that eventually are dying, as a consequence of amosite induced dam-

age, rather than as enhancement of mitogenesis. Conversely, the 2 types of erionite display the lowest cytotoxicity values, combined with DNA neosynthesis and cell proliferation, evaluated both by growth curve and Ki67 marker. Moreover, genotoxic properties of erionite fibers have been reported[8] and are confirmed by our data on 8-OHdG adduct levels, which are significantly higher in cells exposed to erionite fibers of both types. Altogether, these results account for high transforming activity of the few erionite fibers in the pathogenic size range.

Cells from foci induced by erionite displayed the properties of *in vitro* full transformation, *i.e.* changes in morphology, growth in soft agar, high number of passages in culture and increased proliferation rate. Moreover, these cells had autonomous NF-κB, Erk1/2 and Akt activities. Whereas MAPK activity is likely associated to increased cell proliferation rate, NF-κB and Akt are responsible of the increased resistance to cytotoxic agents, as suggested by the rescue of sensitivity upon treatment with specific PI3K and NF-κB inhibitors (not shown). Noteworthy, recently it has been demonstrated a key role for NF-κB in asbestos carcinogenesis in HMC.[18] The presence of activated p65 NF-κB subunit in erionite-induced foci described here is in agreement with these results. Similarly, these cells expressed high levels of HGFR/Met, EGFR and PDGFRβ, suggesting their possible role in sustaining cell survival.

Asbestos is certainly a universally accepted causative agent of MM,[2] although several evidences suggest that SV40 virus may cooperate with asbestos in HMC transformation[23,24] and in the onset of MM.[42] We show here that erionite fibers are able to induce HMC transformation *per se*, regardless SV40 infection. This may explain the high incidence of MM in Cappadocia, a region of Turkey where SV40 virus was never isolated.[3,4,25,26] Erionite is a ubiquitous zeolite, also present in Oregon, USA, where SV40 has been identified in several human specimens.[26] Although amosite is considered a potent human carcinogen, we show here that, according to other similar findings,[23] amosite is not clearly transforming by itself. However, the high level of DNA neosynthesis, as that induced by amosite in these *in vitro* experiments, can induce infidelity of DNA replication and frequent mismatches. Furthermore other agents (such as SV40) can act as critical co-factors, allowing these damaged cells to survive and to progressively acquire biological transformation.

In conclusion, the mineralogical characteristics of erionite fibers (size, surface area and structure) associated with their high transforming capability, highlight the importance of a careful evaluation of the hazard represented by exposure to low concentrations of other similar fibers, to which human beings could be exposed.

Acknowledgements

We thank Dr. J.W. Skidmore (MRC Pneucomoniosis Unit, Llandough Hospital, Penarth, Wales) for providing erionite samples. We also thank Dr. M. Rinaldi for advice on the statistical analysis. This work is part of a G.I. Me. (Gruppo Italiano per lo studio e la terapia del Mesotelioma) network program.

References

1. Mossman BT, Gee JB. Asbestos-related diseases. N Engl J Med 1989;320:1721–30.
2. Mossman BT, Kamp DW, Weitzman SA. Mechanisms of carcinogenesis and clinical features of asbestos-associated cancers. Cancer Invest 1996;14:466–80.
3. Dogan AU, Dogan M, Emri S. Erionite. In: Wexler P. (ed.), Encyclopedia of toxicology, 2nd edn., vol. 2. Oxford: Elsevier, 2005;237–41.
4. Dogan AU, Baris YI, Dogan M, Emri S, Steele I, Elmishad AG, Carbone M. Genetic predisposition to fiber carcinogenesis causes a mesothelioma epidemic in Turkey. Cancer Res 2006;66:5063–8.
5. Okayasu R, Wu L, Hei TK. Biological effects of naturally occurring and man-made fibres: in vitro cytotoxicity and mutagenesis in mammalian cells. Br J Cancer 1999;79:1319–24.
6. Carthew P, Hill RJ, Edwards RE, Lee PN. Intrapleural administration of fibres induces mesothelioma in rats in the same relative order of hazard as occurs in man after exposure. Hum Exp Toxicol 1992;11:530–4.
7. Eborn SK, Aust AE. Effect of iron acquisition on induction of DNA single-strand breaks by erionite, a carcinogenic mineral fiber. Arch Biochem Biophys 1995;316:507–14.
8. Poole A, Brown RC, Turver CJ, Skidmore JW, Griffiths DM. In vitro genotoxic activities of fibrous erionite. Br J Cancer 1983;47:697–705.
9. Wagner JC, Skidmore JW, Hill RJ, Griffiths DM. Erionite exposure and mesotheliomas in rats. Br J Cancer 1985;51:727–30.
10. Long JF, Dutta PK, Hogg BD. Fluorescence imaging of reactive oxygen metabolites generated in single macrophage cells (NR8383) upon phagocytosis of natural zeolite (erionite) fibers. Environ Health Perspect 1997;105:706–11.
11. Janssen YM, Heintz NH, Marsh JP, Borm PJ, Mossman BT. Induction of c-fos and c-jun proto-oncogenes in target cells of the lung and pleura by carcinogenic fibers. Am J Respir Cell Mol Biol 1994;11:522–30.
12. Timblin CR, Guthrie GD, Janssen YW, Walsh ES, Vacek P, Mossman BT. Patterns of c-fos and c-jun proto-oncogene expression, apoptosis, and proliferation in rat pleural mesothelial cells exposed to erionite or asbestos fibers. Toxicol Appl Pharmacol 1998;151:88–97.
13. Johnson GL, Lapadat R. Mitogen-activated protein kinase pathways mediated by ERK, JNK, and p38 protein kinases. Science 2002;298:1911–2.
14. Tsuruo T, Naito M, Tomida A, Fujita N, Mashima T, Sakamoto H, Haga N. Molecular targeting therapy of cancer: drug resistance, apoptosis and survival signal. Cancer Sci 2003;94:15–21.
15. Waddick KG, Uckun FM. Innovative treatment programs against cancer. II. Nuclear factor-κB (NF-κB) as a molecular target. Biochem Pharmacol 1999;57:9–17
16. Berken A, Abel J, Unfried K. β1-integrin mediates asbestos-induced phosphorylation of AKT and ERK1/2 in a rat pleural mesothelial cell line. Oncogene 2003;22:8524–8.
17. Janssen YM, Barchowsky A, Treadwell M, Driscoll KE, Mossman BT. Asbestos induces nuclear factor κ B (NF-κ B) DNA-binding activity and NF-κ B-dependent gene expression in tracheal epithelial cells. Proc Natl Acad Sci USA 1995;92:8458–62.
18. Yang H, Bocchetta M, Kroczynska B, Elmishad AG, Chen Y, Liu Z, Bubici C, Mossman BT, Pass HI, Testa JR, Franzoso G, Carbone M. TNF-α inhibits asbestos-induced cytotoxicity via a NF-κB-dependent pathway, a possible mechanism for asbestos-induced oncogenesis. Proc Natl Acad Sci USA 2006;103:10397–402.
19. Pache JC, Janssen YM, Walsh ES, Quinlan TR, Zanella CL, Low RB, Taatjes DJ, Mossman BT. Increased epidermal growth factor-receptor protein in a human mesothelial cell line in response to long asbestos fibers. Am J Pathol 1998;152:333–40.
20. Bermudez E, Everitt J, Walker C. Expression of growth factor and growth factor receptor RNA in rat pleural mesothelial cells in culture. Exp Cell Res 1990;190:91–8.
21. Cacciotti P, Libener R, Betta P, Martini F, Porta C, Procopio A, Strizzi L, Penengo L, Tognon M, Mutti L, Gaudino G. SV40 replication in human mesothelial cells induces HGF/Met receptor activation: a model for viral-related carcinogenesis of human malignant mesothelioma. Proc Natl Acad Sci USA 2001;98:12032–7.
22. Tolnay E, Kuhnen C, Wiethege T, Konig JE, Voss B, Muller KM. Hepatocyte growth factor/scatter factor and its receptor c-Met are overexpressed and associated with an increased microvessel density in malignant pleural mesothelioma. J Cancer Res Clin Oncol 1998;124:291–6.
23. Bocchetta M, Di Resta I, Powers A, Fresco R, Tosolini A, Testa JR, Pass HI, Rizzo P, Carbone M. Human mesothelial cells are unusually susceptible to simian virus 40-mediated transformation and asbestos cocarcinogenicity. Proc Natl Acad Sci USA 2000;97:10214–19.
24. Cacciotti P, Barbone D, Porta C, Altomare DA, Testa JR, Mutti L, Gaudino G. SV40-dependent AKT activity drives mesothelial cell transformation after asbestos exposure. Cancer Res 2005;65:5256–62.
25. Emri S, Kocagoz T, Olut A, Gungen Y, Mutti L, Baris YI. Simian virus 40 is not a cofactor in the pathogenesis of environmentally induced malignant pleural mesothelioma in Turkey. Anticancer Res 2000;20:891–4.
26. De Rienzo A, Tor M, Sterman DH, Aksoy F, Albelda SM, Testa JR. Detection of SV40 DNA sequences in malignant mesothelioma specimens from the United States, but not from Turkey. J Cell Biochem 2002;84:455–9.
27. Mumpton FA. A reconnaissance study of the association of zeolites with mesothelioma occurrences in central Turkey, United States Department of the Interior Geological Survey, 1979.
28. Dogan M. Sources and types of mineral dust in regions of Turkey with endemic malignant mesothelioma. Indoor Built Environ 2003;12:377–83.

29. Dogan M, Dogan AU. Asbestos mineralogy and health effects. In: Pass HI, Vogelzang NJ, Carbone M. (eds.), Malignant mesothelioma: advances in pathogenesis, diagnosis, and translation therapies. New York: Springer, 2005, 209–25.
30. Kohyama N, Shinohara Y, Suzuki Y. Mineral phases and some reexamined characteristics of the International Union Against Cancer standard asbestos samples. Am J Ind Med 1996;30:515–28.
31. Mossman BT. In vitro approaches for determining mechanisms of toxicity and carcinogenicity by asbestos in the gastrointestinal and respiratory tracts. Environ Health Perspect 1983;53:155–61.
32. Toyokuni S, Sagripanti JL. Association between 8-hydroxy-2′-deoxyguanosine formation and DNA strand breaks mediated by copper and iron. Free Radic Biol Med 1996;20:859–64.
33. Kueng W, Silber E, Eppenberger U. Quantification of cells cultured on 96-well plates. Anal Biochem 1989;182:16–9.
34. Wright WE, Rom WN, Moatamed F. Characterization of zeolite fiber sizes using scanning electron microscopy. Arch Environ Health 1983;38:99–103.
35. Stanton MF, Laynard M, Tegeris A, Miller E, May M, Kent E. Carcinogenicity of fibrous glass: pleural response in the rat in relation to fiber dimension. J Natl Cancer Inst 1977;58:587–603.
36. Becher R, Hetland RB, Refsnes M, Dahl JE, Dahlman HJ, Schwarze PE. Rat lung inflammatory responses after in vivo and in vitro exposure to various stone particles. Inhal Toxicol 2001;13:789–805.
37. Johnson NF, Edwards RE, Munday DE, Rowe N, Wagner JC. Pluripotential nature of mesotheliomata induced by inhalation of erionite in rats. Br J Exp Pathol 1984;65:377–88.
38. Davis JM, Bolton RE, Miller BG, Niven K. Mesothelioma dose response following intraperitoneal injection of mineral fibres. Int J Exp Pathol 1991;72:263–74.
39. Kamp DW, Graceffa P, Pryor WA, Weitzman SA. The role of free radicals in asbestos-induced diseases. Free Radic Biol Med 1992;12:293–315.
40. Marchevsky AM, Wick MR. Current controversies regarding the role of asbestos exposure in the causation of malignant mesothelioma: the need for an evidence-based approach to develop medicolegal guidelines. Ann Diagn Pathol 2003;7:321–32.
41. Maples KR, Johnson NF. Fiber-induced hydroxyl radical formation: correlation with mesothelioma induction in rats and humans. Carcinogenesis 1992;13:2035–9.
42. Mayall FG, Jacobson G, Wilkins R. Mutations of *p53* gene and SV40 sequences in asbestos associated and non-asbestos-associated mesotheliomas. J Clin Pathol 1999;52:291–3.

LUNG CANCER

Preliminary data suggestive of a novel translational approach to mesothelioma treatment: imatinib mesylate with gemcitabine or pemetrexed

Pietro Bertino, Camillo Porta, Dario Barbone, Serena Germano, Sara Busacca, Sabrina Pinato, Giancarlo Tassi, Roberto Favoni, Giovanni Gaudino, Luciano Mutti

See end of article for authors' affiliations

Correspondence to: Dr Giovanni Gaudino, DISCAFF Department and DFBC Center, University of Piemonte Orientale ''A Avogadro'', 28100 Novara, Italy; giovanni.gaudino@unipmn.it

Thorax 2007;**62**:690–695. doi: 10.1136/thx.2006.069872

Received 3 August 2006
Accepted 19 January 2007
Published Online First 22 February 2007

Background: Malignant mesothelioma is a cancer which is refractory to current treatments. Imatinib mesylate is a selective inhibitor of tyrosine kinases such as bcr-abl, c-Kit, c-Fms and platelet derived growth factor receptor β (PDGFRβ). PDGFRβ is often overexpressed in mesothelioma cells and is a therapeutic target for imatinib in some solid tumours. A study was undertaken to assess whether imatinib alone or combined with chemotherapeutic agents may be effective for treating mesothelioma.
Methods: Cultures from mesothelioma MMP, REN and ISTMES2 cell lines were treated with imatinib alone or in combination with a chemotherapeutic agent.
Results: Imatinib induced cytotoxicity and apoptosis selectively on PDGFRβ positive mesothelioma cells via blockade of receptor phosphorylation and interference with the Akt pathway. Of the chemotherapeutic agents tested in combination with imatinib, a synergistic effect was obtained with gemcitabine and pemetrexed.
Conclusions: This study provides a rationale for a novel translational approach to the treatment of mesothelioma which relies on enhancement of tumour chemosensitivity by inhibition of Akt.

Malignant mesothelioma (MMe) is an asbestos-related tumour, the incidence of which is expected to rise dramatically in Europe.[1] In the USA the incidence of MMe has already increased by 90% in the last few years.[2] Because of its biological aggressiveness, MMe is nearly always fatal except in rare less advanced cases, with a median survival of 12.6 months.[3]

A number of growth factors such as hepatocyte growth factor (HGF),[4 5] vascular endothelial growth factor (VEGF)[6 7] and insulin-like growth factor-1 and -2[8] have been shown to play a significant role in the development and progression of MMe. Moreover, several studies have reported a crucial role for platelet derived growth factor (PDGF) A and B in MMe cell growth.[9] A high level of expression of PDGF receptor β (PDGFRβ) was seen in MMe cells but not in normal human mesothelial cells (HMC), mostly expressing PDGFRα.[10] Furthermore, increased expression of PDGF A and B was detected at higher levels in MMe cells than in HMC,[11] and a significant reduction in MMe cell growth or migration was observed by blocking PDGF A and B.[12] Expression of c-Kit on MMe cells has been demonstrated by some authors, although its role in this tumour is controversial.[13–15] Production of macrophage colony stimulating factor (M-CSF) by mesothelial cells has already been reported,[16] and inhibition of c-Fms receptor by imatinib has been demonstrated.[17]

Many cytokines are released in the microenvironment by tumour stromal cells, and PDGF paracrine stimulation has been demonstrated in human tumours, particularly MMe.[18 19] PDGFRβ activated by PDGF B can induce PI3K/Akt signalling[20] which seems to be crucial for the survival of MMe cells.[21]

Imatinib is a selective inhibitor for a subset of tyrosine kinases including bcr-abl, c-Kit, PDGFRβ[22] and c-Fms.[17] PDGF receptors are expressed by several tumour cells and have been identified as potential therapeutic targets for imatinib.[23] In mesothelioma the extent of PDGFRβ positive specimens ranges from about 30% to 45% in different studies.[24 25] Although the therapeutic inefficacy of imatinib monotherapy for mesothelioma has recently been reported,[25 26] combination therapies with imatinib in mice yielded successful results.[27 28] Gemcitabine, cisplatin, etoposide, doxorubicin and, more recently, pemetrexed have been shown to be active in the treatment of MMe. Combined treatment with cisplatin/pemetrexed and cisplatin/gemcitabine have been found to be more effective than each single agent used alone.[29] The aim of the present study is to investigate a translational approach which assesses the possible efficacy of imatinib as a single agent and in combination treatment for MMe.

METHODS

Cell cultures

Mesothelioma cells were derived from pleural effusions and stabilised in culture as continuous cell lines. MMP cells and primary HMC were characterised and cultured as previously described.[5] REN cells were kindly provided by Dr Albelda and ISTMES2 were from the IST cell depository of Genoa (Italy).

Drugs

Imatinib was kindly provided by Novartis (Basel, Switzerland), and gemcitabine and pemetrexed were provided by Lilly (Indianapolis, Indiana, USA). Commercially available cisplatin, doxorubicin and etoposide were obtained from Alexis (Lausen, Switzerland).

Signal transduction

Cells were grown in 0.2% fetal bovine serum (FBS) for 24 h, then pre-incubated for 90 min in the presence or absence of 10 μM imatinib. Purified PDGF (R&D, Milan, Italy), 20 ng/ml, was added to the same medium. Immunoprecipitation and

Abbreviations: HGF, hepatocyte growth factor; HMC, human mesothelial cells; LC_{50}, lethal concentration killing 50% of cells; M-CSF, macrophage colony stimulating factor; MMe, malignant mesothelioma; PDGF, platelet derived growth factor; PDGFRβ, PDGF receptor β; VEGF, vascular endothelial growth factor

immunoblotting were performed as previously described.[5] Antibodies used were: PDGFRβ, phospho-PDGFRβ, c-Kit, c-Fms (Santa Cruz Biotechnology, USA), phospho-Akt-Ser473 (Cell Signaling, USA), phosphotyrosine (UBI, USA) and phospho-Erk1/2 (Sigma, USA). Reactions were detected by the Enhanced Chemiluminescence System (ECL, Amersham, UK).

Cytotoxicity and apoptosis

Subconfluent cells in 96-well plates were exposed for 48 h to medium supplemented with 2% FBS, with or without different drugs at concentrations ranging from 1×10^{-10} M to 1×10^{-3} M. Cell viability was assessed by MTT assay[30] on eight replicas at each concentration point to determine single drug lethal concentration (LC_{50}) values. Normalised cytotoxicity percentages were obtained from the formula: (A_{570} mean values of extracts from treated samples/A_{570} mean values of extracts from untreated control samples) ×100.

LC_{50} values, calculated using Origin software (Microcal Software, USA), were used to draw the theoretical addictivity isobole according to the 50% isobologram method.[31] A series of dose-response curves were then generated for each chemotherapeutic drug as above in the presence of several fixed concentrations of imatinib. The resulting LC_{50} values were plotted on the isobologram for assessment of the hypothetical superadditive effect.

Apoptosis was evaluated by TUNEL analysis (DeadEnd Colorimetric TUNEL System, Promega, USA) following treatment with imatinib, alone or combined with gemcitabine or pemetrexed, and the specific LC_{50} values were determined by MTT analysis in each cell type as follows. MMP: imatinib 3×10^{-7} M, gemcitabine 5×10^{-7} M, pemetrexed 6.5×10^{-6} M; REN: imatinib 1×10^{-6} M, gemcitabine 5×10^{-9} M, pemetrexed 1×10^{-5} M; ISTMES2: imatinib 4×10^{-6} M, gemcitabine 1×10^{-9} M, pemetrexed 5×10^{-6} M. In brief, subconfluent cells plated on glass slide flaskets (NUNC, Rochester, NY, USA) were exposed to medium supplemented with 2% FBS containing the different drugs for 48 h and subsequently fixed in 10% formalin. Biotin-dU positive nuclei were counted on 10 fields with at least 100 cells in the same slide. Values are expressed as the mean (±SE) percentage of positive nuclei of the total counted.

Statistical analysis

For the cytotoxicity assay we performed three separate experiments for each drug and drug combination in the different cell types. Data from each experiment are expressed as mean (SE) values of eight determinations for every concentration point. All mean values from each of the three experiments were used to calculate the curve with the best fit using the Origin software and to calculate the corresponding LC_{50} value with confidence limits by regression analysis. These LC_{50} values were compared using the Student's *t* test with theoretically additive doses and their confidence intervals were calculated as described by Tallarida.[32]

For apoptosis, statistical differences between the theoretical additive effects of the chemotherapeutic agents (gemcitabine or pemetrexed) plus imatinib vs the measured effects of imatinib/chemotherapeutic combinations were evaluated by the Student's *t* test.

In all statistical evaluations the significance threshold is specified in the text.

RESULTS

Expression of PDGFRβ, c-Kit and c-Fms by MMe cells

We evaluated the expression of PDGFRβ, c-Kit (tyrosine kinase receptor for stem cell factor) and c-Fms (M-CSF receptor) by immunoprecipitation and immunoblotting analysis on a panel of eight MMe cell lines. Five of the eight cell lines were positive for PDGFRβ (see fig 1 in supplementary data file available online at http://thorax.bmj.com/supplemental). Of the PDGF receptors, only PDGFRβ (but not PDGFRα) was expressed in MMe cells examined. We selected three MMe cell lines for their different representative expression pattern. PDGFRβ was expressed at a higher level in MMP and REN cells than in ISTMES2 cells, while untransformed HMC did not express the PDGFRβ receptor. The expression of c-Kit and c-Fms occurred at higher levels in MMP cells and was reduced in REN and ISTMES2 cells. HMC only displayed a very low level of c-Fms expression (fig 1A).

Effect of imatinib-mediated PDGFRβ inhibition on Akt

MMe cells positive for PDGFRβ were also tested by immunoprecipitation with PDGFRβ antibodies followed by immunoblotting with phosphotyrosine antibodies after growing cells in low serum conditions. MMe cells displayed negligible levels of tyrosine phosphorylation whereas the addition of recombinant PDGF B increased the receptor phosphorylation of all cells (fig 1B, upper panel). Neither c-Kit nor c-Fms phosphorylation was detectable in the MMe cells (data not shown).

We then determined whether treatment with imatinib could interfere with signalling pathways elicited by this receptor. In low serum conditions, only MMP cells displayed autonomous Akt activity (determined as Ser^{473} phosphorylation) whereas, on stimulation with PDGF, tyrosine phosphorylation of PDGFRβ and Akt phosphorylation were increased but were markedly inhibited by 10 μM imatinib in all MMe cells examined. Basal Erk1/2 activity was slightly enhanced after PDGF in MMP and, to a lesser extent, in REN cells, while both activities were barely affected by treatment with imatinib 10 μM (fig 1B, lower panel).

Conversely, Akt inhibition was complete and comparable to that obtained by treatment with the phosphatidylinositol-3 kinase (PI3K) inhibitor wortmannin at a concentration of 100 nM (fig 1C). Interestingly, Akt activity in MMP cells, expressing also HGFR/Met,[5] was increased by the addition of recombinant HGF (100 ng/ml) but was not affected by imatinib (fig 1D). This indicates a selective blockade of PDGFRβ-dependent Akt signalling by imatinib.

Effect of imatinib on viability of MMe cells expressing PDGFRβ

In view of the crucial role played by Akt in determining survival of HMC and MMe cells,[21] we postulated that imatinib could negatively affect the viability of PDGFRβ-positive MMe cells. After incubation for 48 h with up to 100 μM imatinib, cell viability tested by the MTT assay was markedly decreased with a LC_{50} of 1.84×10^{-5} M, 1.89×10^{-5} M and 2.05×10^{-5} M for MMP, REN and ISTMES2 cells, respectively. Gemcitabine and pemetrexed have already been shown to be particularly effective in combination with cisplatin for MMe chemotherapy.[29] We therefore tested the cytotoxic effect induced by these two agents in the presence of different concentrations of imatinib. As expected, gemcitabine and pemetrexed killed MMe cells in a dose-dependent manner. The presence of imatinib modified the profile of the dose-response curves with a shift towards lower LC_{50} values and a decrease in the fraction of drug-resistant cells (fig 2A).

We did not observe any evidence of PDGFRβ phosphorylation/activation by either gemcitabine or pemetrexed (see fig 2 in supplementary data file available online at http://thorax.bmj.com/supplemental), as recently reported for epidermal growth factor receptor.[33]

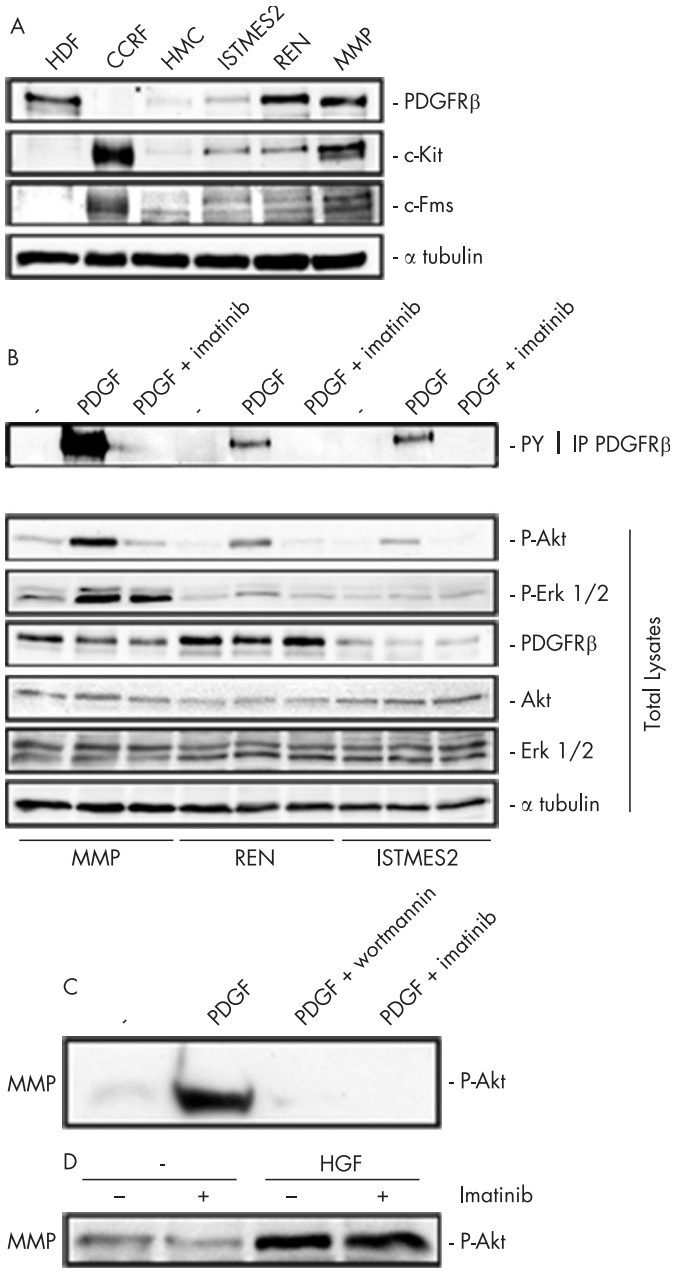

Figure 1 Expression of platelet derived growth factor receptor β (PDGFRβ) in malignant mesothelioma (MMe) cells. (A) Immunoblotting with PDGFRβ, c-Kit and c-Fms antibodies on human mesothelial cells (HMC) and three representative MMe cell lines. Controls: human dermal fibroblasts (HDF) expressing PDGFRβ and CCRF, CCRF-HSB-2, human leukaemic lymphoblast cells expressing c-Kit and c-Fms. (B) Immunoprecipitation with PDGFRβ antibodies followed by immunoblotting with phosphotyrosine antibodies (upper panel); immunoblotting with the indicated antibodies on whole lysates (lower panel). In both panels MMP, REN and ISTMES2 cells were in low serum (−) or stimulated with PDGF in the presence or absence of 10 μM imatinib or (C) 100 nM wortmannin. (D) Immunoblotting with P-Akt (P-Ser 473) antibodies of MMP cells stimulated by 50 ng/ml hepatocyte growth factor (HGF) in the presence or absence of 10 μM imatinib.

Synergy of imatinib with gemcitabine and pemetrexed in inducing MMe cell death

Activation of tyrosine kinase receptors by ligands induces PI3K and Akt activities, exerting several biological effects including increased cell survival with relevant effects on human carcinogenesis.[34] We have recently shown that Akt plays a major survival role for MMe cells.[21] Therefore, based on the clear-cut toxic effect induced by imatinib on MMe cells mediated by the inhibition of the PI3K/Akt pathway, we hypothesised that this inhibitor may also reinforce cytotoxicity generated by other cytotoxic agents.

Combined treatments of imatinib with other chemotherapeutic drugs were therefore analysed by the isobologram plot method.[31] Interestingly, only imatinib/gemcitabine and imatinib/pemetrexed combinations showed a significant synergism in reducing MMP ($p \leqslant 0.001$) and REN (ranging from $p \leqslant 0.01$ to $p \leqslant 0.001$) cell viability compared with the effects observed with single agents alone. This was revealed by inserting all LC_{50} values on a concave upward curve below the isoeffective plot (fig 2B). In REN cells the synergistic effect is still appreciable, although to a lower extent, while in ISTMES2 cells the effect of imatinib in combination with other chemotherapeutic agents was significantly antagonistic (ranging from $p \leqslant 0.05$ to $p \leqslant 0.001$).

The effectiveness of these combined treatments was confirmed when cell death was investigated by TUNEL analysis. The combination of imatinib with gemcitabine or pemetrexed induced a significant increase in apoptosis ($p \leqslant 0.001$) compared with the theoretical additive effect of each chemotherapeutic agent with imatinib (table 1). No synergistic effect was observed with any of the other chemotherapeutic drugs (results not shown). Interestingly, the concentrations of the single agents used in the combined treatment were much lower than those obtained at therapeutic dosages.

DISCUSSION

We describe here some preclinical results which provide a rationale for a novel combined approach to MMe treatment via inhibition of PDGFRβ signalling. Our findings on cultured cells are in accordance with previous evidence of PDGFRβ expression in MMe cells and a lack of expression in normal HMC.[10] With regard to the relevance of PDGFRβ expression in vivo, the percentage of positive specimens reported is in the range of 30–45% in the different studies reported.[24 25] These data therefore offer a rationale for testing the tyrosine kinase inhibitor imatinib on PDGFRβ activity in MMe cells.

Autocrine or paracrine mechanisms may explain the activation of PDGFRβ in vivo. An autocrine loop has been described as an activating mechanism leading to tyrosine kinase receptor activity in MMe cells,[5] and the stromal microenvironment has been shown to be a fundamental source of activating ligands for PDGFR in human tumours.[35] Tyrosine phosphorylation of this receptor in MMP and REN cells is inhibited by imatinib, leading to cytotoxic effects and addressing the role of downstream PI3K/Akt survival signalling.

We and others have shown that Akt activation in MMe cells is a crucial signalling pathway which contributes to the MMe malignant phenotype.[21 36] Even though this is also dependent on the activity of several other tyrosine kinase receptors, our findings show that specific interference with the PDGFRβ-dependent pathway causes an increase in cell chemosensitivity.

Preclinical studies on several human solid tumours have confirmed the efficacy of imatinib as a cytotoxic agent.[37–40] In chronic myeloid leukaemia and gastrointestinal stromal tumour the carcinogenic role of the fusion protein BCR-ABL[39] and activating mutations of c-Kit,[41] respectively, predict a clinical response to imatinib. Conversely, in MMe, two recent negative reports gave clear evidence that imatinib monotherapy is ineffective.[25 26] On the other hand, combined treatment with imatinib and different chemotherapeutic agents has been shown to be effective in mice.[27 28]

Our results clearly indicate that PDGFRβ expression in MMe cells is essential for sensitivity to imatinib and for the synergy observed between imatinib and gemcitabine or pemetrexed.

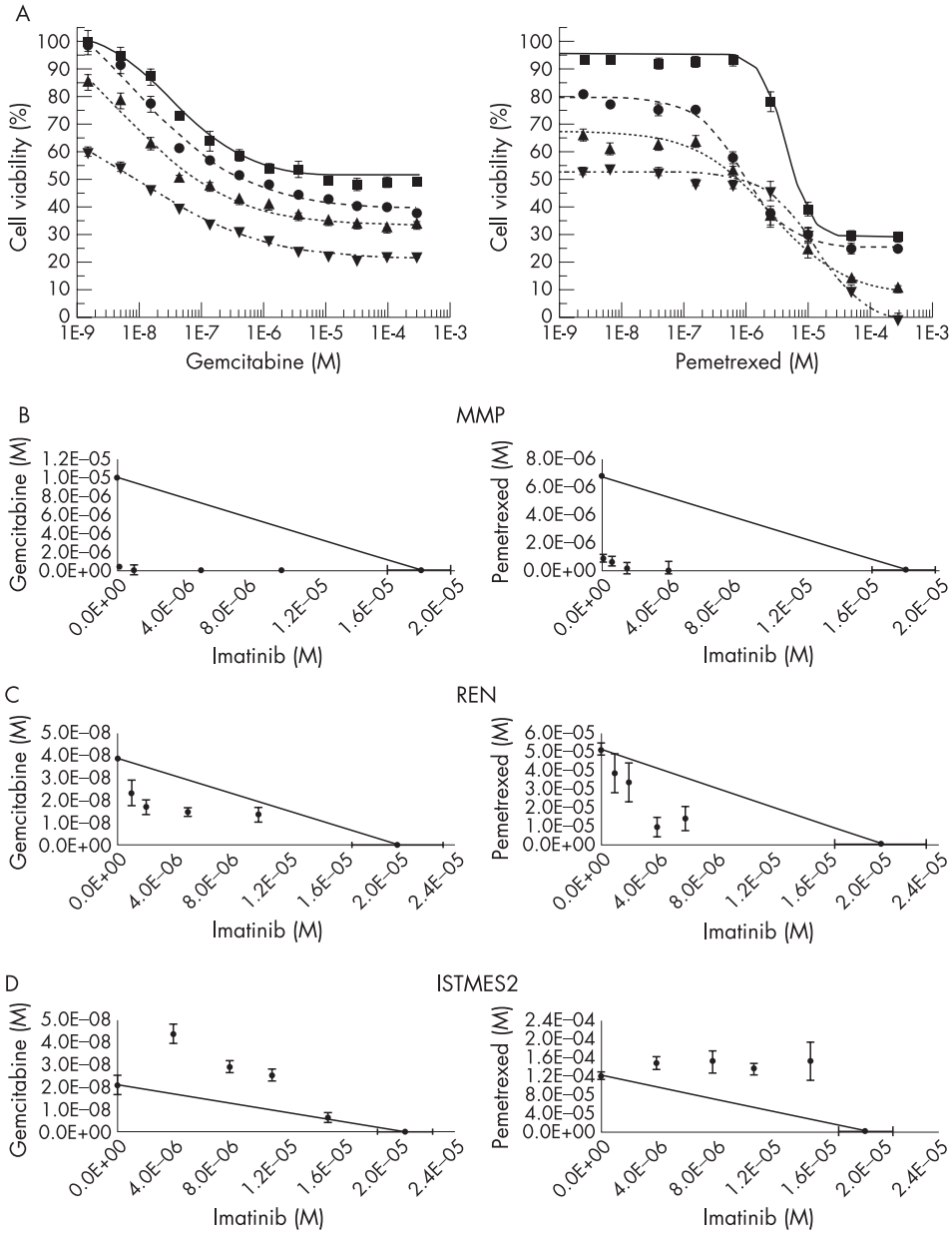

Figure 2 Synergy of imatinib with gemcitabine and pemetrexed. (A) Dose-effect curves of cell viability for gemcitabine (left) and pemetrexed (right) in the presence of different concentrations of imatinib. For the imatinib/gemcitabine combination: ●, 1×10^{-7} M; ▲, 2.5×10^{-6} M; ▼, 1×10^{-4} M. For the imatinib/pemetrexed combination: ●, 3×10^{-7} M; ▲, 6×10^{-7} M; ▼, 1.5×10^{-6} M. Representative data from three experiments conducted with eight determinations for each point. Points represent mean (±SE) percentage . (B–D) 50% isobologram plot for imatinib in combination with gemcitabine (left) and pemetrexed (right) on MMP, REN and ISTMES2 cells. Points are mean (±SE) 50% lethal concentration (LC_{50}) calculated by regression analysis.

However, when all three receptors sensitive to imatinib and upstream of the PI3K/Akt pathway are co-expressed in the same cell type, as in MMP, the synergistic effect is higher than in REN cells where only two of them are expressed (PDGFRβ and c-Kit).

Gemcitabine and pemetrexed are known to be active on MMe cells[42] and their combination with imatinib has intriguing implications. In particular, the synergism shown in this study indicates that very low doses of chemotherapeutic agents should be sufficient to exert a therapeutic effect.

Table 1 TUNEL analysis of apoptosis induced in malignant mesothelioma (MMe) cells by single drugs or by drug combinations

Treatment	MMP	REN	ISTMES2
Imatinib	1.10 (0.35)	1.00 (0.23)	1.70 (0.19)
Gemcitabine	1.58 (0.42)	3.07 (0.51)	2.80 (0.32)
Pemetrexed	0.98 (0.47)	1.04 (0.26)	1.00 (0.26)
Imatinib + gemcitabine	5.34 (0.40)*	9.72 (0.48)*	1.02 (0.48)*
Imatinib + pemetrexed	8.48 (0.40)*	4.72 (0.26)*	0.04 (0.26)*

Data are expressed as the mean (SE) percentage of biotin-dU positive nuclei for 100 counted cells at a magnification of 100×. The values for each treatment were subtracted from untreated control values. Different concentrations of drugs were used, as described in the Methods section.
*$p \leqslant 0.001$, difference between theoretical additive effects of chemotherapeutics (gemcitabine or pemetrexed) + imatinib vs measured effects of imatinib/chemotherapeutic combinations.

Given our previous findings,[21] the mechanism underlying the observed in vitro synergy is probably imatinib-dependent PDGFRβ inhibition which, in turn, leads to Akt inactivation resulting in sensitisation of MMe cells to low chemotherapeutic concentrations. However, it is conceivable that other biological effects could play a role in humans. Reduction of the intratumoral interstitial fluid pressure and increased uptake of chemotherapeutics by imatinib have been shown in vivo.[27] In addition, imatinib has been shown to interfere with VEGF expression and associated neoangiogenesis.[43]

Although some progress has been made in the treatment of MMe, the results are still unsatisfactory and MMe remains an ideal field in which to test new therapeutic approaches.[42] Our work on the synergy between imatinib and chemotherapeutic drugs active in MMe provides a strong rationale for a new approach to the treatment of this disease and will be evaluated further in early phase clinical trials.

ACKNOWLEDGEMENTS

The authors thank Dr Patrizia Morbini, Institute of Pathology, San Matteo University Hospital, Pavia, Italy and also Dr M Rinaldi for advice on statistical analysis.

Further details are shown in figs 1 and 2 in the supplementary data file available online at http://thorax.bmj.com/supplemental.

Authors' affiliations

Pietro Bertino, Dario Barbone, Serena Germano, Sara Busacca, Sabrina Pinato, Giovanni Gaudino, DISCAFF Department and DFB Center, University of Piemonte Orientale ''A Avogadro'', Novara, Italy
Camillo Porta, Medical Oncology, IRCCS San Matteo University Hospital, Pavia, Italy
Giancarlo Tassi, Chest Medicine Unit, Brescia Hospital, Brescia, Italy
Roberto Favoni, National Cancer Institute, Genoa, Italy
Luciano Mutti, Local Health Unit, 11 Piemonte, Italy

This work was supported by research grants to GG from AIRC (Associazione Italiana per la Ricerca sul Cancro), MARF (Mesothelioma Applied Research Foundation) and the Buzzi Foundation (Casale Monferrato, Italy). This work is part of G.I.Me. (Gruppo Italiano per lo Studio e la Terapia del Mesotelioma) network program.

Competing interests: None declared.

GG and LM contributed equally to the study.

REFERENCES

1 **Peto J**, Decarli A, La Vecchia C, *et al.* The European mesothelioma epidemic. *Br J Cancer* 1999;**79**:666–72.
2 **Treasure T**, Sedrakyan A. Pleural mesothelioma: little evidence, still time to do trials. *Lancet* 2004;**364**:1183–5.
3 **Pass HI**, Vogelzang N, Hahn S, *et al.* Malignant pleural mesothelioma. *Curr Probl Cancer* 2004;**28**:93–174.
4 **Klominek J**, Baskin B, Liu Z, *et al.* Hepatocyte growth factor/scatter factor stimulates chemotaxis and growth of malignant mesothelioma cells through c-met receptor. *Int J Cancer* 1998;**76**:240–9.
5 **Cacciotti P**, Libener R, Betta P, *et al.* SV40 replication in human mesothelial cells induces HGF/Met receptor activation: a model for viral-related carcinogenesis of human malignant mesothelioma. *Proc Natl Acad Sci USA* 2001;**98**:12032–7.
6 **Strizzi L**, Catalano A, Vianale G, *et al.* Vascular endothelial growth factor is an autocrine growth factor in human malignant mesothelioma. *J Pathol* 2001;**193**:468–75.
7 **Cacciotti P**, Strizzi L, Vianale G, *et al.* The presence of simian-virus 40 sequences in mesothelioma and mesothelial cells is associated with high levels of vascular endothelial growth factor. *Am J Respir Cell Mol Biol* 2002;**26**:189–93.
8 **Hoang CD**, Zhang X, Scott PD, *et al.* Selective activation of insulin receptor substrate-1 and -2 in pleural mesothelioma cells: association with distinct malignant phenotypes. *Cancer Res* 2004;**64**:7479–85.
9 **Garlepp MJ**, Leong CC. Biological and immunological aspects of malignant mesothelioma. *Eur Respir J* 1995;**8**:643–50.
10 **Langerak AW**, van der Linden-van Beurden CA, Versnel MA. Regulation of differential expression of platelet-derived growth factor alpha- and beta-receptor mRNA in normal and malignant human mesothelial cell lines. *Biochim Biophys Acta* 1996;**1305**:63–70.
11 **Pogrebniak HW**, Lubensky IA, Pass HI. Differential expression of platelet derived growth factor-beta in malignant mesothelioma: a clue to future therapies? *Surg Oncol* 1993;**2**:235–40.
12 **Klominek J**, Baskin B, Hauzenberger D. Platelet-derived growth factor (PDGF) BB acts as a chemoattractant for human malignant mesothelioma cells via PDGF receptor beta-integrin alpha3beta1 interaction. *Clin Exp Metastasis* 1998;**16**:529–39.
13 **Horvai AE**, Li L, Xu Z, *et al.* c-Kit is not expressed in malignant mesothelioma. *Mod Pathol* 2003;**16**:818–22.
14 **Butnor KJ**, Burchette JL, Sporn TA, *et al.* The spectrum of Kit (CD117) immunoreactivity in lung and pleural tumors: a study of 96 cases using a single-source antibody with a review of the literature. *Arch Pathol Lab Med* 2004;**128**:538–43.
15 **Catalano A**, Rodilossi S, Rippo MR, *et al.* Induction of stem cell factor/c-Kit/slug signal transduction in multidrug-resistant malignant mesothelioma cells. *J Biol Chem* 2004;**279**:46706–14.
16 **Lanfrancone L**, Boraschi D, Ghiara P, *et al.* Human peritoneal mesothelial cells produce many cytokines (granulocyte colony-stimulating factor (CSF), granulocyte-monocyte-CSF, macrophage-CSF, interleukin-1 (IL-1), and IL-6) and are activated and stimulated to grow by IL-1. *Blood* 1992;**80**:2835–42.
17 **Taylor JR**, Brownlow N, Domin J, *et al.* FMS receptor for M-CSF (CSF-1) is sensitive to the kinase inhibitor imatinib and mutation of Asp-802 to Val confers resistance. *Oncogene* 2006;**25**:147–51.
18 **Kindler HL**. Moving beyond chemotherapy: novel cytostatic agents for malignant mesothelioma. *Lung Cancer* 2004;**45**(Suppl 1):S125–7.
19 **Shih AH**, Holland EC. Platelet-derived growth factor (PDGF) and glial tumorigenesis. *Cancer Lett* 2006;**232**:139–47.
20 **Johnson MD**, Okedli E, Woodard A, *et al.* Evidence for phosphatidylinositol 3-kinase-Akt-p7S6K pathway activation and transduction of mitogenic signals by platelet-derived growth factor in meningioma cells. *J Neurosurg* 2002;**97**:668–75.
21 **Cacciotti P**, Barbone D, Porta C, *et al.* SV40-dependent AKT activity drives mesothelial cell transformation after asbestos exposure. *Cancer Res* 2005;**65**:5256–62.
22 **George D**. Platelet-derived growth factor receptors: a therapeutic target in solid tumors. *Semin Oncol* 2001;**28**(5 Suppl 17):27–33.
23 **Abou-Jawde R**, Choueiri T, Alemany C, *et al.* An overview of targeted treatments in cancer. *Clin Ther* 2003;**25**:2121–37.
24 **Roberts F**, Harper CM, Downie I, *et al.* Immunohistochemical analysis still has a limited role in the diagnosis of malignant mesothelioma. A study of thirteen antibodies. *Am J Clin Pathol* 2001;**116**:253–62.
25 **Porta C**, Mutti L, Tassi G. Negative results of an Italian Group for Mesothelioma (G.I.Me.) pilot study of single-agent imatinib mesylate in malignant pleural mesothelioma. *Cancer Chemother Pharmacol* 2007;**59**:149–50.
26 **Mathy A**, Baas P, Dalesio O, *et al.* Limited efficacy of imatinib mesylate in malignant mesothelioma: a phase II trial. *Lung Cancer* 2005;**50**:83–6.
27 **Pietras K**, Stumm M, Hubert M, *et al.* STI571 enhances the therapeutic index of epothilone B by a tumor-selective increase of drug uptake. *Clin Cancer Res* 2003;**9**:3779–87.
28 **Yokoi K**, Sasaki T, Bucana CD, *et al.* Simultaneous inhibition of EGFR, VEGFR, and platelet-derived growth factor receptor signaling combined with gemcitabine produces therapy of human pancreatic carcinoma and prolongs survival in an orthotopic nude mouse model. *Cancer Res* 2005;**65**:10371–80.
29 **Tomek S**, Manegold C. Chemotherapy for malignant pleural mesothelioma: past results and recent developments. *Lung Cancer* 2004;**45**(Suppl 1): S103–19.
30 **Mosmann T**. Rapid colorimetric assay for cellular growth and survival: application to proliferation and cytotoxicity assays. *J Immunol Methods* 1983;**65**:55–63.
31 **Tallarida RJ**. Drug synergism: its detection and applications. *J Pharmacol Exp Ther* 2001;**298**:865–72.
32 **Tallarida RJ**. Statistical analysis of drug combinations for synergism. *Pain* 1992;**49**:93–7.
33 **Feng FY**, Varambally S, Tomlins SA, *et al.* Role of epidermal growth factor receptor degradation in gemcitabine-mediated cytotoxicity. *Oncogene* 2007;**17**:3431–9.
34 **Stein RC**. Prospects for phosphoinositide 3-kinase inhibition as a cancer treatment. *Endocr Relat Cancer* 2001;**8**:237–48.
35 **Sawyers C**. Targeted cancer therapy. *Nature* 2004;**432**:294–7.
36 **Rascoe PA**, Cao X, Daniel JC, *et al.* Receptor tyrosine kinase and phosphoinositide-3 kinase signaling in malignant mesothelioma. *J Thorac Cardiovasc Surg* 2005;**130**:393–400.
37 **Krystal GW**, Honsawek S, Litz J, *et al.* The selective tyrosine kinase inhibitor STI571 inhibits small cell lung cancer growth. *Clin Cancer Res* 2000;**6**:3319–26.
38 **Wang WL**, Healy ME, Sattler M, *et al.* Growth inhibition and modulation of kinase pathways of small cell lung cancer cell lines by the novel tyrosine kinase inhibitor STI 571. *Oncogene* 2000;**19**:3521–8.
39 **Druker BJ**, Sawyers CL, Kantarjian H, *et al.* Activity of a specific inhibitor of the BCR-ABL tyrosine kinase in the blast crisis of chronic myeloid leukemia and acute lymphoblastic leukemia with the Philadelphia chromosome. *N Engl J Med* 2001;**344**:1038–42.
40 **Gonzalez I**, Andreu EJ, Panizo A, *et al.* Imatinib inhibits proliferation of Ewing tumor cells mediated by the stem cell factor/KIT receptor pathway, and sensitizes

cells to vincristine and doxorubicin-induced apoptosis. *Clin Cancer Res* 2004;**10**:751–61.
41 **Heinrich MC**, Corless CL, Demetri GD, *et al.* Kinase mutations and imatinib response in patients with metastatic gastrointestinal stromal tumor. *J Clin Oncol* 2003;**21**:4342–9.
42 **Vogelzang NJ**, Porta C, Mutti L. New agents in the management of advanced mesothelioma. *Semin Oncol* 2005;**32**:336–50.
43 **Beppu K**, Jaboine J, Merchant MS, *et al.* Effect of imatinib mesylate on neuroblastoma tumorigenesis and vascular endothelial growth factor expression. *J Natl Cancer Inst* 2004;**96**:46–55.

Imatinib Mesylate Enhances Therapeutic Effects of Gemcitabine in Human Malignant Mesothelioma Xenografts

Pietro Bertino,[1] Federica Piccardi,[2] Camillo Porta,[4] Roberto Favoni,[3] Michele Cilli,[2] Luciano Mutti,[5] and Giovanni Gaudino[1]

Abstract

Purpose: Platelet-derived growth factor receptor β (PDGFRβ), frequently activated in malignant mesothelioma, is a promising cancer therapeutic target. Imatinib mesylate (STI571; Glivec) is a selective inhibitor of tyrosine kinases as bcr-abl, c-kit, c-fms, and PDGFRβ and enhances tumor drug uptake by reducing the interstitial fluid pressure. We previously showed that imatinib mesylate synergizes with gemcitabine and pemetrexed in PDGFRβ-positive mesothelioma cells. Here, we aimed at investigating these combined treatments in a novel mesothelioma model.

Experimental Design: REN mesothelioma cells, infected with a lentiviral vector carrying the *luciferase* gene, were injected in the peritoneum of severe combined immunodeficient mice. This model allowed imaging of live animals treated with pemetrexed or gemcitabine chemotherapeutics, or with imatinib mesylate alone, as well as with a combination of gemcitabine and imatinib mesylate.

Results: We show here that, consistent with our previous *in vitro* studies, gemcitabine inhibited tumor growth, whereas pemetrexed was ineffective, even at the highest dosage tested. Compared with monotreatment, the combination of gemcitabine with imatinib mesylate led to a further tumor growth inhibition and improved mice survival, by a decrease rate of tumor cell proliferation and an increase in number of apoptotic tumor cells.

Conclusions: Imatinib mesylate enhances the therapeutic response to gemcitabine, in accordance with our previous *in vitro* data. These *in vivo* results validate imatinib mesylate and gemcitabine as a combination treatment of malignant mesothelioma, also in view of its known positive effects on tumor drug uptake. These evidences provide the rationale for the currently ongoing clinical trials.

Malignant mesothelioma is an asbestos-related malignant tumor, whose incidence will increase dramatically in the next decade (1). Due to its biological aggressiveness, the median survival is about 12 months, with a yearly death toll of 2,000 to 3,000 in the United States and about 1,000 in the United Kingdom (2). Hence, the urgency of new drug development to improve the clinical course of the disease.

The continuing increase in the incidence of malignant mesothelioma has been associated with the widespread use of asbestos in the past century. The mechanism of asbestos carcinogenesis has been linked to the activation of proinflammatory cytokines and nuclear factor-κB (3).

Only a fraction of about 5% of the subjects exposed to high levels of asbestos develop malignant mesothelioma (4). This finding suggests that additional factors, such as SV40 infection and genetic predisposition, may render these individuals to be more susceptible to asbestos carcinogenicity (5–7).

Moreover, SV40 and asbestos were shown to be cocarcinogens in hamster (8, 9) and caused malignant transformation of human mesothelial cells through activation of protein kinase B (10).

Interstitial hypertension is a feature of most solid tumors (11). The notion that increased interstitial fluid pressure (IFP) acts as a barrier for drug delivery into the tumor has recently found experimental support. Lowering of the IFP or, by other means, improving the transcapillary pressure gradient has been shown to increase the uptake of low molecular weight compounds, gases, and tumor-targeting antibodies (12). In some instances, it was further shown that the decrease in tumor IFP and the increase in tumor drug uptake were paralleled by an enhanced effect of anticancer therapy (13). Thus, there is

Authors' Affiliations: [1]Department of Chemical, Food, Pharmaceutical and Pharmacological Sciences and Drug and Food Biotechnology Center, University of Piemonte Orientale "A. Avogadro," Novara, Italy; [2]Animal Model Facility, National Cancer Institute and [3]Laboratory of Experimental Pharmacology, National Cancer Institute, Genoa, Italy; [4]Medical Oncology, Istituto di Ricovero e Cura a Carattere Scientifico/San Matteo University Hospital, Pavia, Italy; and [5]Department of Medicine, Local Health Unit 11, Piemonte, Italy

Received 6/5/07; revised 8/24/07; accepted 9/26/07.

Grant support: Mesothelioma Applied Research Foundation, Regione Piemonte, and Associazione Italiana per la Ricerca sul Cancro (G. Gaudino); Buzzi Foundation for the study of Mesothelioma; and Italian Group for the Study and Therapy for Mesothelioma (G. Gaudino).

The costs of publication of this article were defrayed in part by the payment of page charges. This article must therefore be hereby marked *advertisement* in accordance with 18 U.S.C. Section 1734 solely to indicate this fact.

Note: L. Mutti and G. Gaudino contributed equally to this work.

Requests for reprints: Giovanni Gaudino, Department of Chemical, Food, Pharmaceutical and Pharmacological Sciences and Drug and Food Biotechnology Center, University of Piemonte Orientale "A. Avogadro," Via Bovio 6, 28100 Novara, Italy. Phone: 39-0321-375815; Fax: 39-0321-375821; E-mail: giovanni.gaudino@unipmn.it.

doi:10.1158/1078-0432.CCR-07-1388

mounting evidence that poor drug delivery from the bloodstream into the tumor interstitium can be augmented by adjuvant therapy with substances that lower the IFP.

Several findings underscore the crucial role of platelet-derived growth factor (PDGF) A and B in malignant mesothelioma cell growth (reviewed in 14). High expression level of PDGF receptor β (PDGFRβ) was shown in malignant mesothelioma cells, but not in normal human mesothelial cells, mostly expressing PDGFRα (15). Furthermore, increased expression of PDGF A and B were detected at higher levels in malignant mesothelioma cells compared with human mesothelial cells (16), and a significant reduction in malignant mesothelioma cell growth or migration was observed by blocking PDGF A and PDGF B (17). Many cytokines are released in the microenvironment by tumor stromal cells (18), and PDGF paracrine stimulation has been shown in human tumors and malignant mesothelioma in particular (19, 20). PDGFRβ activated by PDGF B can induce phosphatidylinositol-3-OH/protein kinase B signaling (21), which contributes to malignant mesothelioma cells survival (10). Inhibition of PDGFRβ was recently shown to lower the tumor IFP in different tumor models. The reduction in tumor IFP was paralleled by an increased tumor uptake of paclitaxel (Taxol) or epothilone B and a concomitant enhancement of the therapeutic efficacy (11 – 13). In mesothelioma, the extent of specimens positive for PDGFRβ expression ranges from about 30% to 45% in different studies (22, 23). Hence, large patient group might therefore benefit from therapeutic targeting of this signaling pathway.

Imatinib mesylate is a selective inhibitor for a subset of tyrosine kinases, including bcr-abl, c-Kit, PDGFRβ (24), as well as c-Fms (25). However, the therapeutic inefficacy of imatinib mesylate monotherapy for mesothelioma has been recently reported (22, 26), although we recently showed that imatinib mesylate synergizes with gemcitabine and pemetrexed selectively on PDGFRβ-positive mesothelioma cells (27).

Gemcitabine, cisplatin, etoposide, doxorubicin, and more recently, pemetrexed have been confirmed to be active for malignant mesothelioma treatment. Combined therapy of platin used with pemetrexed or gemcitabine has been shown to be more effective than each single agent alone (28).

On the other hand, combination therapies with imatinib mesylate yielded successful results in other human solid tumors grown in mice, indicating the involvement of PDGFRβ signaling in the regulation of tumor IFP and *trans*-vascular transport (13, 29). In the present preclinical study, we have investigated the effects of oral imatinib mesylate administration combined with i.p. injection of gemcitabine on the inhibition of the progressive growth of human malignant mesothelioma cells into the peritoneum of severe combined immunodeficient (SCID) mice.

Materials and Methods

Cell cultures. MMP mesothelioma cells were characterized and cultured as previously described (30). REN mesothelioma cells, kindly provided by Dr. Albelda (University of Pennsylvania, Philadelphia, PA), were cultured in Ham's F-12 medium (Sigma) supplemented with 10% fetal bovine serum (Invitrogen) and maintained at 37°C in a 5% CO_2 – humidified atmosphere.

REN/luc luminescent cells and REN/green fluorescent protein fluorescent cells were derived from the REN cell line that was transduced with the lentiviral vector pRRL.sin.PPT.CMV, which was precarrying either a bioluminescent genetic marker (luciferase) or a fluorescent marker (green fluorescent protein).

Drugs. Imatinib mesylate was kindly provided by Novartis; gemcitabine and pemetrexed were provided by Lilly.

Animals. C.B-17-SCID or athymic *nu/nu* mice (female, 6-8 weeks old; Charles River) received i.p. injections of 1×10^6 mesothelioma cells (MMP, REN, or REN-transduced cells) in 0.5 mL of Ham's F-12 medium. To assess tumor dimension and localization of luminescent cells after anesthetization and i.p. injections of 0.3 mL of 15 mg/mL D-luciferin, bioluminescence signals of Ren/luc-inoculated mice were monitored using the IVIS system 100 series (Xenogen Corp.). Regions of interest were identified around the tumor sites and were quantified as total photon counts using Living Image software (Xenogen Corp.). The values of tumor sizes were obtained, subtracting luminescence signals of each weekly measurement by the first measurement on the 10th day after inoculation, and these were expressed as the average of all values for every treatment group.

To evaluate the treatments toxicity, mice were weighed at the start and end of treatments. Mice were killed and necropsied when tumor developments caused severe ascites limiting the animals mobility. Survival was evaluated by the Kaplan-Meier method. Mice that were used for histologic studies were excluded from statistical analysis of death.

All animal experiments were done in accordance with institutional animal committee guidelines. Mice were maintained and handled under aseptic conditions, and animals were allowed access to food and water *ad libitum*.

Administration of drugs. An elapse of a period of 10 days was allowed for the formation of detectable tumor nodules by IVIS imaging. Mice were then weighed and stratified into each treatment groups of seven animals. Treatment protocols were done from the 13th day to the 27th day, and mice were analyzed weekly by IVIS imaging to assess tumor growth until the 43rd day. Imatinib mesylate, alone or combined with gemcitabine, was given daily by oral gavage at 100 or 200 mg/kg as a single oral dose in 200 μL of PBS. Gemcitabine alone or in combination with imatinib was injected in different treatment groups i.p. at 120, 60, and 30 mg/kg every 3rd day for five doses, a regimen that was established previously as a well-tolerated dosage for SCID mice (31). Pemetrexed was injected in different treatment groups i.p. at 250 and 150 mg/kg on days 15th to 19th and 22nd to 26th, as previously reported in human tumor xenografts (32). Gemcitabine treatment started on the 3rd day after the beginning of imatinib treatment and, when injected on the same day, imatinib mesylate was given 1 to 2 h before chemotherapeutics (13). Control mice received i.p. injection of PBS and administration of DMSO, by oral gavage, diluted at 1:20 in water, as vehicles.

Necroscopy procedures for histologic studies. After tumor cell injection, at day 28th, one mouse from each group was killed and necropsied. Tumors growing in the peritoneum were excised, and one part of the tumor tissue was fixed in formalin and embedded in paraffin.

Immunohistochemical staining of proliferating cells and terminal deoxynucleotidyl transferase-mediated nick end labeling analysis. Sections were deparaffinized in xylene, dehydrated with alcohol, and rehydrated in PBS. Endogenous peroxidases were blocked with 3% hydrogen peroxide in PBS. After 1 h of incubation at room temperature with Ki67 antibodies (Neomarkers), biotin-streptavidin immunostaining was done with UltraVision (Labvision Co.) detection system, according to the manufacturer's instructions. Apoptosis was evaluated in parallel sections by terminal deoxynucleotidyl transferase-mediated nick end labeling (TUNEL) analysis (DeadEnd Colorimetric TUNEL system; Promega). For quantification of Ki67 expression and apoptosis, the number of positive cells was counted in 10 random fields at ×100 magnification.

Statistical analysis. Tumor dimensions, body weight changes, Ki67-positive cells, and TUNEL-positive cells were compared using the

Student's t test among different groups, as indicated in the text. Data from each experiment were expressed as mean ± SE. Survival was computed by the Kaplan-Meier method and compared by the log-rank test.

Experiments were repeated, and every vehicle treated groups from each evaluation was joint as a unique group for statistical analysis. In all significant evaluations, the threshold was specified in the text, and all statistical tests were two sided.

Results

Injection of engineered human mesothelioma cells allowed tumor imaging in SCID mice. To verify the efficacy of malignant mesothelioma xenografts, SCID or *nu/nu* (athymic, nude) mice were inoculated i.p. with 1×10^6 REN or MMP malignant mesothelioma cells, both expressing PDGFRβ. After 20 days, all SCID mice inoculated with REN cells developed abdominal palpable lumps. The autopsy confirmed the presence of histopathologically determined malignant mesothelioma in all animals. None of the nude mice nor SCID mice that were inoculated with MMP cells developed malignant mesothelioma. REN mesothelioma cells were transduced with a lentiviral vector, carrying either *luciferase* gene (REN/luc) or *green fluorescent protein* gene (REN/GFP), to allow imaging in live mice. After 30 days from inoculation, the animals were sacrificed. Autopsy revealed the occurrence of numerous peritoneal nodules (Fig. 1). IVIS imaging of malignant mesothelioma cells revealed a high fluorescence background in REN/GFP–inoculated mice. The detection of xenografts obtained with luciferase-transduced cells REN/luc was more sensitive and accurate. Therefore, we selected the REN/luc system for subsequent experiments.

Treatment with imatinib mesylate was ineffective on REN mesothelioma cell growth in SCID mice. The effects of treatment with imatinib mesylate were investigated on our newly established malignant mesothelioma model of SCID mice injected with REN/luc cells. Ten days after cell inoculation, tumor incidence in the peritoneal cavity was 100% in all treatment groups detailed below.

Two doses of imatinib mesylate were used (200 and 100 mg/kg). Interestingly, treatment with the higher dose (200 mg/kg) produced a significant increase of tumor dimensions compared with control-treated animals at each weekly observation ($P < 0.01$); however, survival was not influenced. Instead, a dose of 100 mg/kg imatinib mesylate did not induce any significant increase in tumor mass, compared with the control group, which also did not influence survival (Fig. 2A).

The toxicity of treatment regimens was assessed, evaluating changes of mice body weights during the drugs administration. Mice treated with 100 mg/kg of imatinib mesylate had weight gain comparable with controls. However, higher doses (200 mg/kg) resulted in a significant lower weight gain compared with controls ($P < 0.001$), suggesting toxicity (Table 1).

Survival rate was analyzed using the Kaplan-Meier method (Fig. 2B). These data indicated 100 mg/kg of imatinib mesylate as the more suitable dosage for combination therapies.

Pemetrexed is not effective on the malignant mesothelioma SCID mouse model. To investigate the efficacy of pemetrexed in our xenograft mesothelioma model, we stratified mice injected with REN/luc mesothelioma cells into the following three treatment groups: (*a*) control, vehicle alone; (*b*) 250 mg/kg pemetrexed alone; and (*c*) 150 mg/kg pemetrexed alone. We previously showed that REN mesothelioma cells respond to pemetrexed, with a LC_{50} of about 50 μmol/L, whereas LC_{50} for gemcitabine is about 40 nmol/L on the same cells (27). *In vivo* treatment with pemetrexed 150 mg/kg displayed a significant effect only at the end of the experiments ($P < 0.001$). Injection of 250 mg/kg pemetrexed surprisingly produced an unexpected significant increase of tumor mass compared with controls for the entire time span of the experiments ($P < 0.01$; Fig. 3A).

The toxicity of treatment regimens based on mice body weight changes is shown in Table 1. Pemetrexed given at 150 mg/kg led to an increase of mice body weight at lesser extent than vehicle treated mice ($P < 0.001$). The dose of 250 mg/kg induced a significant positive body weight variation compared with control animals ($P < 0.001$), but both treatments did not significantly improve survival (Fig. 3B). Despite the discrepancy from the established pemetrexed efficacy in mesothelioma treatment, these data were in accordance with our previous *in vitro* results where the REN mesothelioma cells were much more resistant to pemetrexed than gemcitabine (27). Moreover, the combination of pemetrexed at 250 mg/kg with

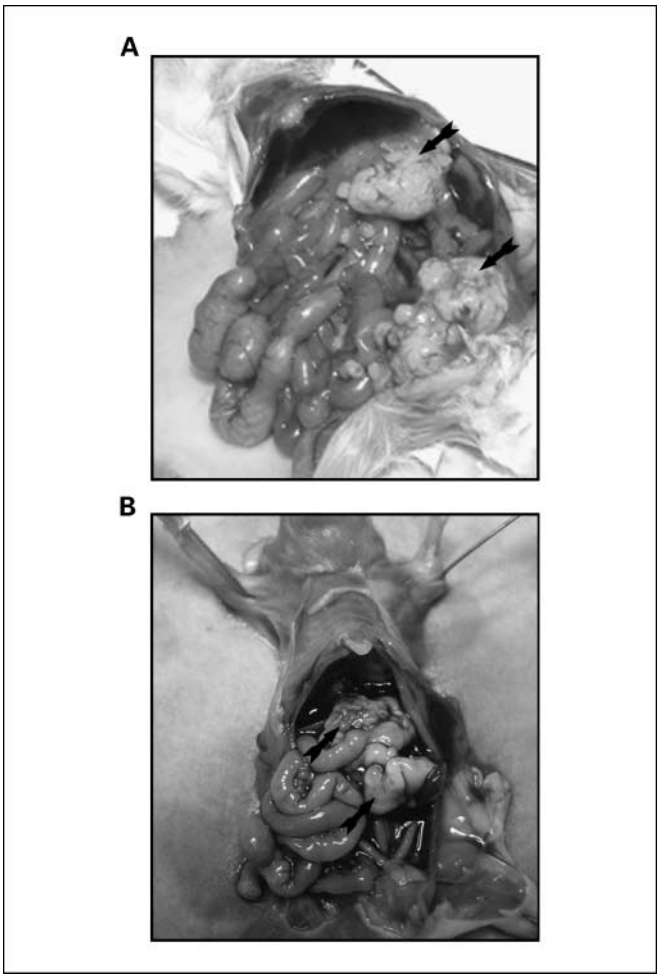

Fig. 1. REN cells transduced with lentiviral vector induced recognizable tumors in SCID mouse. Necroscopy of SCID mice inoculated with REN cells transduced with lentiviral vector carrying *green fluorescent protein* gene (*A*) or *luciferase* gene (*B*), after 56 d from implantation. Black arrows, tumor masses.

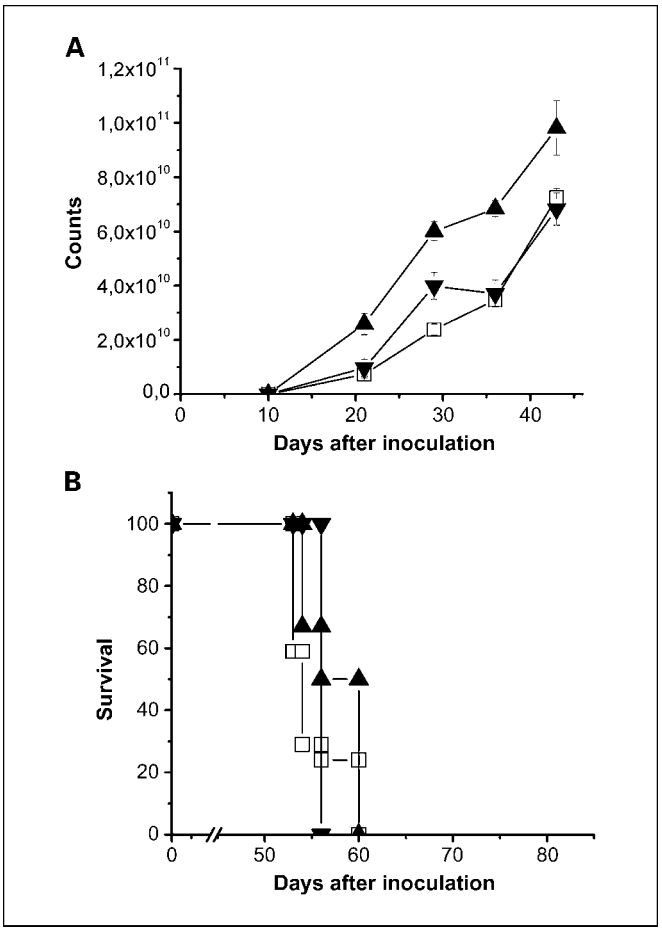

Fig. 2. Imatinib mesylate allows disease progress in mice inoculated with REN/luc cells. *A,* quantitative analysis of the whole-body total photon counts of vehicle (□) and imatinib mesylate – treated mice at doses of 200 mg/kg (▲) and 100 mg/kg (▼). *B,* mice were i.p. inoculated with 1×10^6 REN/luc mesothelioma cells on day 0. Imatinib mesylate was given daily, starting on day 13 and continuing until day 27. Mice were killed when tumor development caused severe ascites limiting the animals mobility. Survival analysis of mice treated either with vehicle (□), 200 mg/kg imatinib mesylate (▲), or with 100 mg/kg imatinib mesylate (▼) was done by the Kaplan-Meier method and compared by the log-rank test.

imatinib mesylate at 100 mg/kg reduced tumor masses, body weights, and survivals to values similar to those of control tumor-bearing mice (data not shown).

Combination with imatinib mesylate reinforces gemcitabine antitumor efficacy in the malignant mesothelioma SCID mouse model. We recently reported a synergistic cytotoxic interaction between imatinib mesylate and gemcitabine on REN mesothelioma cells (27). To verify these results in the *in vivo* model, we injected SCID mice with REN/luc luminescent cells eliciting xenograft tumor formation. We then stratified tumor-bearing animals into groups receiving control vehicle or gemcitabine at doses of 120, 60, and 30 mg/kg. These doses have been reported to be well tolerated in mice by specific pharmacokinetics studies (33). Dose-dependent tumor growth inhibition was observed with gemcitabine alone (data not shown), although the treatment with the dosages of 120 mg/kg was toxic (Table 1) and had to be discontinued.

Subsequently, 100 mg/kg imatinib mesylate was given in combination with dosages of gemcitabine of 60 and 30 mg/kg. The results were compared with those obtained in the same experiment with mice injected with vehicle or gemcitabine alone at the same dosages.

Gemcitabine at 60 mg/kg significantly delayed tumor growth after the end of treatment (36th day), whereas the dosage of 30 mg/kg revealed a smaller growth delay with a significant tumor volume reduction only at the end of IVIS observations, on 43rd day after tumor inoculation ($P < 0.001$; Fig. 4A). Imatinib mesylate at 100 mg/kg combined with gemcitabine at 60 mg/kg caused a statistically significant suppression of tumor growth at the end of the observation period, compared with the gemcitabine monotreatment group ($P < 0.001$; Fig. 4A and C). Combination treatment of imatinib mesylate with the lowest effective dosage of gemcitabine of 30 mg/kg induced only a weak improvement of the chemotherapeutic drug effect, which was not statistically significant (data not shown). Body weight changes resulting from different treatments are illustrated in Table 1. The dosages of 60 and 30 mg/kg of gemcitabine, alone or combined with imatinib mesylate, did not cause any weight loss, in contrast to the weight loss caused by gemcitabine alone at 120 mg/kg. Mice treated with gemcitabine alone at 60 and 30 mg/kg did not reveal any survival improvement. Instead, combination of imatinib mesylate with gemcitabine at 60 mg/kg significantly improved the survival of treated mice ($P < 0.01$). At day 60, vehicle-treated mice displayed a severe ascite, whereas the ascite of mice under this combined treatment was clearly reduced, in accordance with data on tumor dimensions (Fig. 4B and D). Survival of mice treated with imatinib mesylate in combination with the lowest effective dose of gemcitabine (30 mg/kg) was not modified, compared with monotreatment at the same dose (data not shown).

These results are consistent with those recently observed *in vitro* (27) and clearly indicate that *in vivo* combination of imatinib mesylate plus gemcitabine 60 mg/kg leads to an improved antitumor activity, compared with the antitumor activity of each agent alone.

Histopathologic analysis of cell growth and apoptosis in human mesothelioma xenografts. Tissues from tumors growing in the

Table 1. Body weight changes on SCID mice measured after each treatment

Treatment	Body weight variation (%)*	
Vehicle	+	8.71 ± 0.24
200 mg/kg imatinib mesylate	+	4.32 ± 0.18
100 mg/kg imatinib mesylate	+	14.47 ± 0.42
120 mg/kg gemcitabine	-	13.41 ± 0.21
60 mg/kg gemcitabine	+	12.70 ± 0.31
30 mg/kg gemcitabine	+	6.22 ± 0.17
250 mg/kg pemetrexed	+	16.51 ± 0.34
150 mg/kg pemetrexed	+	6.27 ± 0.13
60 mg/kg gemcitabine + 100 mg/kg imatinib mesylate	+	9.52 ± 0.24
30 mg/kg gemcitabine + 100 mg/kg imatinib mesylate	+	9.49 ± 0.12

*Mice were weighed before and after treatments to evaluate resultant toxicity. Data are expressed as the mean percentage of weight change ± SE.

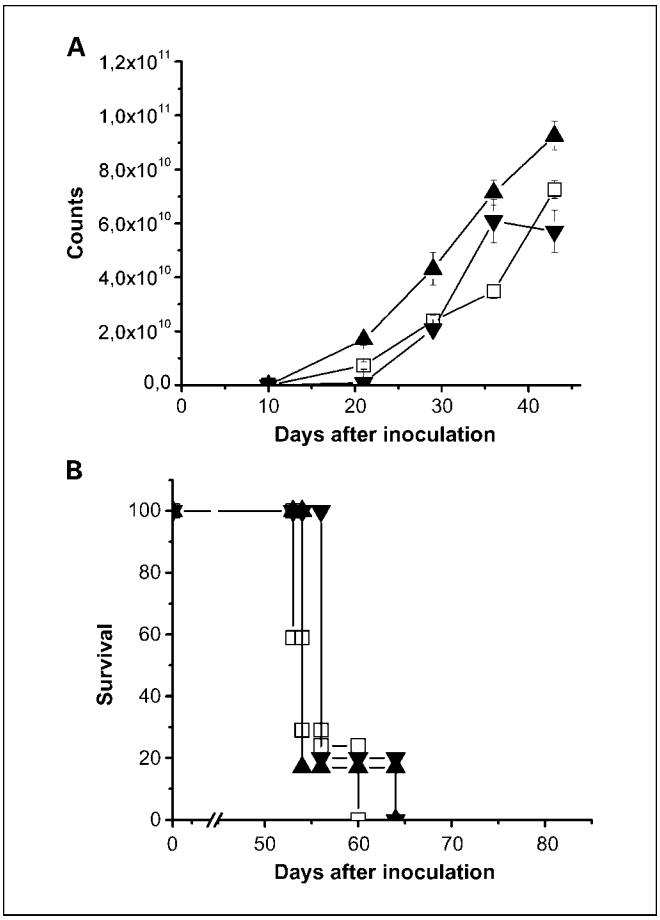

Fig. 3. Tumor growth analysis and survival of pemetrexed-treated xenogafts. *A,* quantitative analysis of the tumor cell emissions in mice treated with pemetrexed at 250 mg/kg (▲), 150 mg/kg (▼), or with vehicle (□). *B,* survival analysis on groups of mice treated with pemetrexed at doses of 250 mg/kg (▲) or 150 mg/kg (▼) compared with vehicle treatment (□).

mice peritoneum were excised, formalin fixed, paraffin embedded, and analyzed for cell proliferation and apoptosis. Cell proliferation was evaluated by Ki67 staining (proliferating cell nuclear antigen). In tumors from control mice, the median number of Ki67-positive cells was 17.9 ± 3.0. Treatment with imatinib mesylate at 100 mg/kg alone or gemcitabine at 60 mg/kg alone did not alter the number of dividing Ki67-positive cells, whereas a significant decrease of Ki67-positive cells was found in tumors treated with combination regimens, compared with chemotherapeutic monotreatments ($P < 0.001$; Fig. 5). Pemetrexed given at 250 mg/kg induced, if compared with vehicle injection, a statistically significant increase of cell proliferation (data not shown), in accordance with tumor growth data shown in Fig. 3A.

The evaluation of apoptosis in the malignant mesothelioma mice tumors was done by TUNEL assay. In tumors from vehicle-treated mice, the median number of apoptotic tumor cells was minimal (3.4 ± 0.8). The number of apoptotic cells in tumors from mice treated with imatinib mesylate given alone was not significantly different from control mice tumors. Therapy with gemcitabine at 60 mg/kg given alone induced a significant increase of apoptotic cell number when compared with vehicle injection ($P < 0.001$), and combination with imatinib mesylate further significantly improved this figures ($P < 0.05$; Fig. 5).

Discussion

In this article, using a new animal model of human malignant mesothelioma, we show that the combination of gemcitabine with a specific tyrosine kinase inhibitor can enhance the efficacy of mesothelioma treatment. We recently reported that imatinib mesylate synergizes with gemcitabine and pemetrexed selectively on PDGFRβ-positive mesothelioma cells (27). The results shown here confirm our preclinical results obtained *in vitro* and provide further evidences with relevant translational implications. To validate this novel approach to malignant mesothelioma therapy, we established a mouse model injecting REN mesothelioma cells on the peritoneum of SCID mice, carrying either a *luciferase* gene or a *green fluorescent protein* gene to allow imaging by IVIS imaging system.

A major advantage of a marking system using a charged coupled device camera is the ability to evaluate tumor dimension changes sequentially over time in the same living animal. This ability obviates the need to euthanize multiple cohorts of animals at each required time point. This approach reduces potential animal-to-animal variance and allows long term studies (34).

Studies *in vivo* on malignant mesothelioma showed that percentage of positive specimens for PDGFRβ expression is in the range of 30% to 45%, depending on the different studies (22, 23). Either autocrine or paracrine mechanisms may cause the activation of PDGFRβ *in vivo*. Several autocrine loops have been described as an activating mechanism leading to tyrosine kinase receptor activity in malignant mesothelioma cells (30, 35, 36), and stromal microenvironment has been shown to be a fundamental source of activating ligands for PDGFR in human tumors (18). We have shown that tyrosine phosphorylation of PDGFRβ in MMP and REN cells is inhibited by imatinib mesylate, leading to cytotoxic effects (27).

Preclinical studies on several human solid tumors revealed the efficacy of imatinib mesylate as a cytotoxic agent (37, 38). In opposition, two recent negative reports gave clear evidence that imatinib mesylate monotherapy is ineffective for malignant mesothelioma (22, 26). On the other hand, combined therapy of imatinib mesylate with different chemotherapeutic agents has been shown effective. A number of studies reported a decreased interstitial hyper pressure in tumor stroma provoked by the imatinib mesylate inhibition of PDGFR signaling, which in turn improves the drug delivery, enhancing the effects of chemotherapeutic reagents (11–13, 29).

In analogy to the previous clinical observations (22), we show here that imatinib mesylate as a single treatment has limited effect on the inhibition of tumor growth and prolongation of survival. On the other hand, the combination of imatinib mesylate with gemcitabine significantly lowers the number of Ki67-positive cells and increases the number of apoptotic tumor cells, causing inhibition of tumor growth and prolonged survival. This therapeutic effect was significantly more efficient than that of gemcitabine monotreatment. Furthermore, in the regimens where gemcitabine was well-tolerated, imatinib

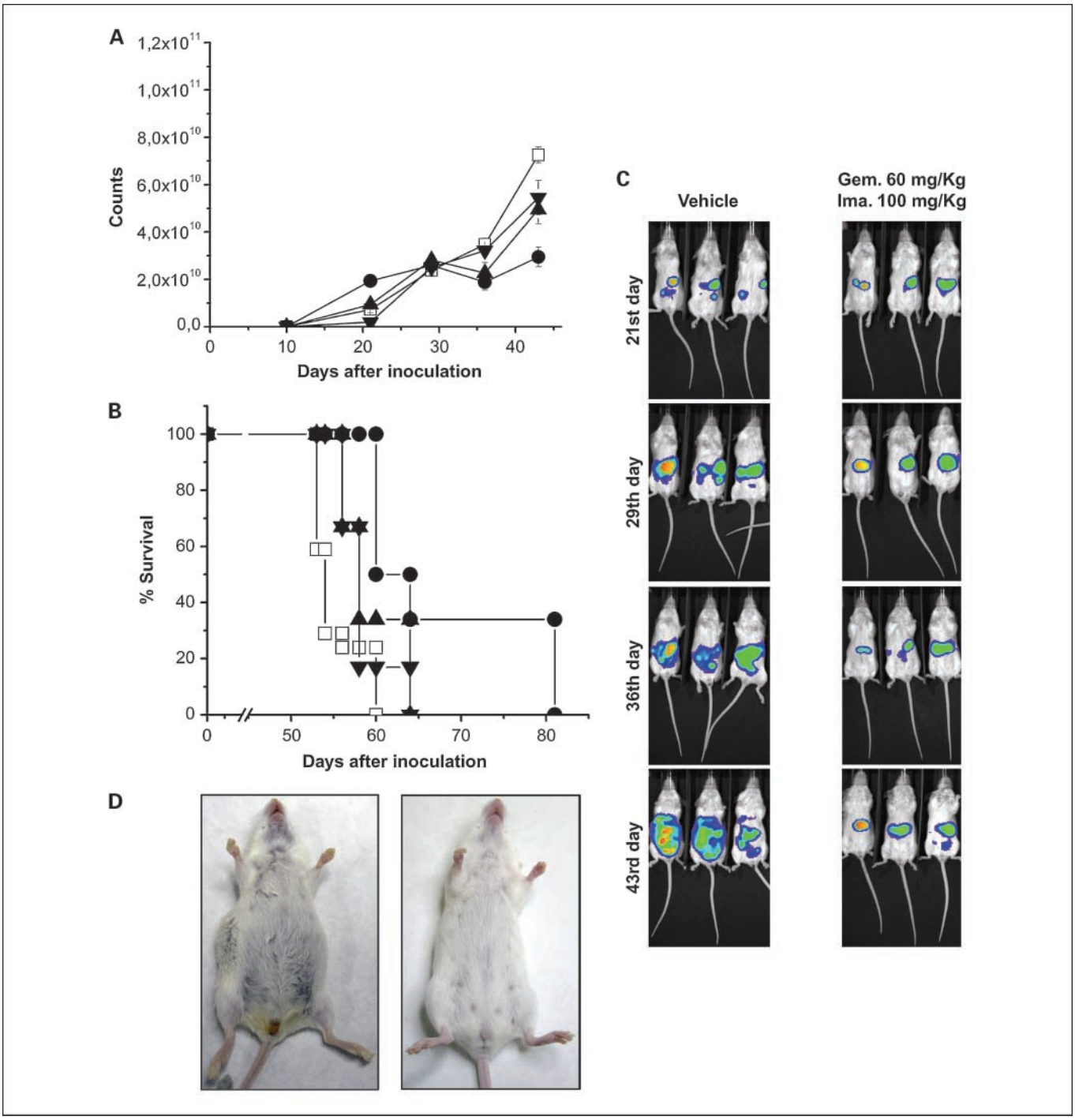

Fig. 4. Imatinib mesylate enhances gemcitabine therapy in human mesothelioma xenografts. *A,* tumor inhibition by 60 mg/kg gemcitabine combined with imatinib mesylate (●), compared with vehicle (□) and gemcitabine given alone at 60 mg/kg (▲) and 30 mg/kg (▼). *B,* survival analysis of SCID mice treated with vehicle (□), 60 mg/kg gemcitabine (▲), 30 mg/kg gemcitabine (▼), or 60 mg/kg gemcitabine combined with 100 mg/kg imatinib mesylate (●). *C,* REN/luc cells were i.p. inoculated into SCID mice on day 0. Treatments were from 13th day to 27th day, and mice were analyzed weekly by IVIS imaging to assess tumor growth. After 43 d, IVIS imaging system showed that combined treatment with gemcitabine 60 mg/kg and imatinib mesylate 100 mg/kg partially suppressed tumor growth on the peritoneal cavity compared with control mice. *D,* on 60th day, vehicle-treated mice (*left*) have severe ascite compared with mice under combined treatment (60 mg/kg gemcitabine – 100 mg/kg imatinib mesylate; *right*).

mesylate treatment did not cause toxicity, compared with gemcitabine monotreatments, as judged by body weight.

In conclusion, previous findings from our group and others (10, 13, 27, 29) showed that imatinib mesylate inhibited PDGFRβ, which in turn led to protein kinase B inactivation, resulting in malignant mesothelioma cell sensitization to low chemotherapeutic concentrations. The previously established synergism *in vitro* was improved *in vivo* where imatinib mesylate is presumably also able to decrease the tumor IFP, therefore increasing the uptake of cytotoxic drugs into the

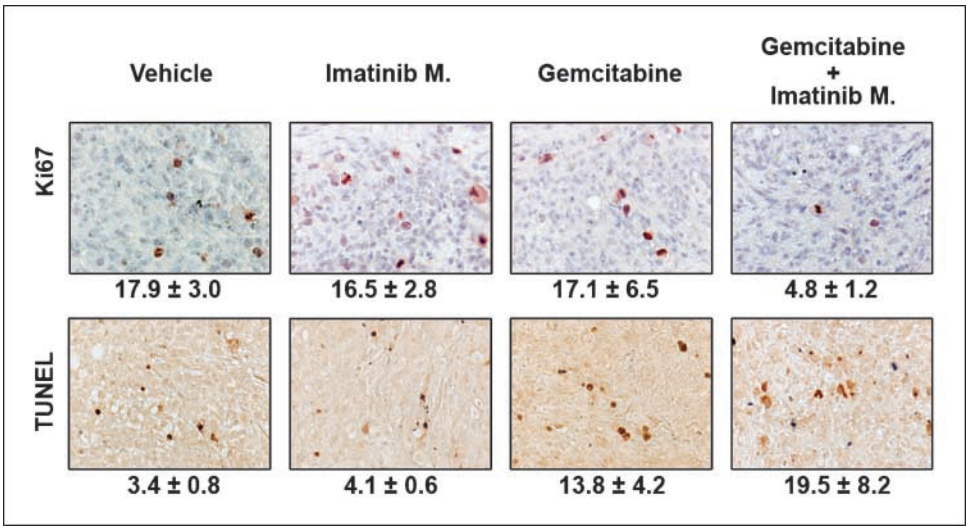

Fig. 5. Analysis of cell proliferation (Ki67) and apoptosis (TUNEL). Mice were treated with vehicle, 100 mg/kg imatinib mesylate, 60 mg/kg gemcitabine alone, or combined with 100 mg/kg imatinib mesylate. Tumors were resected and processed for immunohistochemical evaluation of Ki67 and TUNEL as described in Materials and Methods.

tumor stroma. Consequently, our successful results on the novel human malignant mesothelioma animal model, confirming our *in vitro* findings, show that imatinib mesylate enhances gemcitabine effects on malignant mesothelioma.

The proof of principle established by our present work and by a clinical pilot study[6] allowed us to design a phase II clinical trial currently ongoing.

Acknowledgments

We thank the Buzzi Foundation (Casale Monferrato, Italy) for financial help, Gruppo Italiano Mesotelioma for logistic support, the San Paolo foundation for the IVIS imaging system, Dr. Albelda for kindly providing REN cells, Dr. M. Rinaldi for advice on the statistical analysis, and Zeyana Rivera for editing the manuscript.

[6] L. Mutti, personal communication.

References

1. Peto J, Decarli A, La Vecchia C, Levi F, Negri E. The European mesothelioma epidemic. Br J Cancer 1999; 79:666–72.
2. Pass HI, Lott D, Lonardo F, et al. Asbestos exposure, pleural mesothelioma, and serum osteopontin levels. N Engl J Med 2005;353:1564–73.
3. Yang H, Bocchetta M, Kroczynska B, et al. TNF-α inhibits asbestos-induced cytotoxicity via a NF-κB-dependent pathway, a possible mechanism for asbestos-induced oncogenesis. Proc Natl Acad Sci U S A 2006;103:10397–402.
4. Rizzo P, Bocchetta M, Powers A, et al. SV40 and the pathogenesis of mesothelioma. Semin Cancer Biol 2001;11:63–71.
5. Carbone M, Emri S, Dogan AU, et al. A mesothelioma epidemic in Cappadocia: scientific developments and unexpected social outcomes. Nat Rev Cancer 2007;7: 147–54.
6. Dogan AU, Baris YI, Dogan M, et al. Genetic predisposition to fiber carcinogenesis causes a mesothelioma epidemic in Turkey. Cancer Res 2006;66:5063–8.
7. Cutrone R, Lednicky J, Dunn G, et al. Some oral poliovirus vaccines were contaminated with infectious SV40 after 1961. Cancer Res 2005;65:10273–9.
8. Kroczynska B, Cutrone R, Bocchetta M, et al. Crocidolite asbestos and SV40 are cocarcinogens in human mesothelial cells and in causing mesothelioma in hamsters. Proc Natl Acad Sci U S A 2006;103:14128–33.
9. Bocchetta M, Di Resta I, Powers A, et al. Human mesothelial cells are unusually susceptible to simian virus 40-mediated transformation and asbestos cocarcinogenicity. Proc Natl Acad Sci U S A 2000;97:10214–9.
10. Cacciotti P, Barbone D, Porta C, et al. SV40-dependent AKT activity drives mesothelial cell transformation after asbestos exposure. Cancer Res 2005;65: 5256–62.
11. Pietras K, Ostman A, Sjoquist M, et al. Inhibition of platelet-derived growth factor receptors reduces interstitial hypertension and increases transcapillary transport in tumors. Cancer Res 2001;61:2929–34.
12. Pietras K, Rubin K, Sjoblom T, et al. Inhibition of PDGF receptor signaling in tumor stroma enhances antitumor effect of chemotherapy. Cancer Res 2002; 62:5476–84.
13. Pietras K, Stumm M, Hubert M, et al. STI571 enhances the therapeutic index of epothilone B by a tumor-selective increase of drug uptake. Clin Cancer Res 2003;9:3779–87.
14. Garlepp MJ, Leong CC. Biological and immunological aspects of malignant mesothelioma. Eur Respir J 1995;8:643–50.
15. Langerak AW, van der Linden-van Beurden CA, Versnel MA. Regulation of differential expression of platelet-derived growth factor α- and β-receptor mRNA in normal and malignant human mesothelial cell lines. Biochim Biophys Acta 1996;1305:63–70.
16. Pogrebniak HW, Lubensky IA, Pass HI. Differential expression of platelet derived growth factor-β in malignant mesothelioma: a clue to future therapies? Surg Oncol 1993;2:235–40.
17. Klominek J, Baskin B, Hauzenberger D. Platelet-derived growth factor (PDGF) BB acts as a chemoattractant for human malignant mesothelioma cells via PDGF receptor β-integrin α3β1 interaction. Clin Exp Metastasis 1998;16:529–39.
18. Sawyers C. Targeted cancer therapy. Nature 2004; 432:294–7.
19. Shih AH, Holland EC. Platelet-derived growth factor (PDGF) and glial tumorigenesis. Cancer Lett 2005; 232:139–47.
20. Yu J, Ustach C, Kim HR. Platelet-derived growth factor signaling and human cancer. J Biochem Mol Biol 2003;36:49–59.
21. Johnson MD, Okedli E, Woodard A, Toms SA, Allen GS. Evidence for phosphatidylinositol 3-kinase-Akt-p7S6K pathway activation and transduction of mitogenic signals by platelet-derived growth factor in meningioma cells. J Neurosurg 2002;97:668–75.
22. Porta C, Mutti L, Tassi G. Negative results of an Italian Group for Mesothelioma (G.I.Me.) pilot study of single-agent imatinib mesylate in malignant pleural mesothelioma. Cancer Chemother Pharmacol 2007; 59:149–50.
23. Roberts F, Harper CM, Downie I, Burnett RA. Immunohistochemical analysis still has a limited role in the diagnosis of malignant mesothelioma. A study of thirteen antibodies. Am J Clin Pathol 2001;116: 253–62.
24. George D. Platelet-derived growth factor receptors: a therapeutic target in solid tumors. Semin Oncol 2001;28:27–33.
25. Taylor JR, Brownlow N, Domin J, Dibb NJ. FMS receptor for M-CSF (CSF-1) is sensitive to the kinase inhibitor imatinib and mutation of Asp-802 to Val confers resistance. Oncogene 2006;25:147–51.
26. Mathy A, Baas P, Dalesio O, van Zandwijk N. Limited efficacy of imatinib mesylate in malignant mesothelioma: a phase II trial. Lung Cancer 2005; 50:83–6.
27. Bertino P, Porta C, Barbone D, et al. Preliminary data suggestive of a novel translational approach to mesothelioma therapy: imatinib mesylate with gemcitabine or pemetrexed. Thorax 2007;62:690–5.
28. Tomek S, Manegold C. Chemotherapy for malignant pleural mesothelioma: past results and recent developments. Lung Cancer 2004;45 Suppl 1: S103–19.
29. Yokoi K, Sasaki T, Bucana CD, et al. Simultaneous inhibition of EGFR, VEGFR, and platelet-derived growth factor receptor signaling combined with gemcitabine produces therapy of human pancreatic

carcinoma and prolongs survival in an orthotopic nude mouse model. Cancer Res 2005;65:10371–80.

30. Cacciotti P, Libener R, Betta P, et al. SV40 replication in human mesothelial cells induces HGF/Met receptor activation: a model for viral-related carcinogenesis of human malignant mesothelioma. Proc Natl Acad Sci U S A 2001;98:12032–7.

31. Braakhuis BJ, Ruiz van Haperen VW, Boven E, Veerman G, Peters GJ. Schedule-dependent antitumor effect of gemcitabine in *in vivo* model system. Semin Oncol 1995;22:42–6.

32. Teicher BA, Chen V, Shih C, et al. Treatment regimens including the multitargeted antifolate LY231514 in human tumor xenografts. Clin Cancer Res 2000;6:1016–23.

33. Braakhuis BJ, Ruiz van Haperen VW, Welters MJ, Peters GJ. Schedule-dependent therapeutic efficacy of the combination of gemcitabine and cisplatin in head and neck cancer xenografts. Eur J Cancer 1995;31A:2335–40.

34. Yoshimitsu M, Sato T, Tao K, et al. Bioluminescent imaging of a marking transgene and correction of Fabry mice by neonatal injection of recombinant lentiviral vectors. Proc Natl Acad Sci U S A 2004;101:16909–14.

35. Strizzi L, Catalano A, Vianale G, et al. Vascular endothelial growth factor is an autocrine growth factor in human malignant mesothelioma. J Pathol 2001;193:468–75.

36. Pass HI, Mew DJ, Carbone M, Donington JS, Baserga R, Steinberg SM. The effect of an antisense expression plasmid to the IGF-1 receptor on hamster mesothelioma proliferation. Dev Biol Stand 1998;94:321–8.

37. Gonzalez I, Andreu EJ, Panizo A, et al. Imatinib inhibits proliferation of Ewing tumor cells mediated by the stem cell factor/KIT receptor pathway, and sensitizes cells to vincristine and doxorubicin-induced apoptosis. Clin Cancer Res 2004;10:751–61.

38. Druker BJ, Sawyers CL, Kantarjian H, et al. Activity of a specific inhibitor of the BCR-ABL tyrosine kinase in the blast crisis of chronic myeloid leukemia and acute lymphoblastic leukemia with the Philadelphia chromosome. N Engl J Med 2001;344:1038–42.

CONCLUSIONS

I consider the PhD school in Molecular Medicine an exciting experience in which I had the opportunity to develop knowledge on different topics regards MM. In the first three years, under the supervision of Prof. G. Gaudino, I studied in deep some carcinogenic processes that bring to development of MM. Using primary mesothelial cells obtained from healthy donors, I investigated the molecular mechanism changes consequently to exposure with different kind of putative carcinogens for MM such as SV40, asbestos and erionite. The role of SV40 in MM is still controversial and it seems unlikely that SV40 contributes to the MM development independently of asbestos because humans are much more resistant than rodents to viral carcinogens and because most MM develop in asbestos-exposed individuals. Two proteins mediate the effects of SV40 infection: large T antigen (TAg) and small t antigen (tAg). TAg binds and inactivates a set of tumor suppressor genes, including *Rb*, *p107*, *p130*, and *p53*. Although the precise role of tAg is not well understood, it seems to enhance transformation by TAg. This may occurs through its ability to inhibit the protein phosphatase complex (PP2A) [27]. Both TAg and tAg act on proteins that are key regulators of cell cycle checkpoints, and loss of their normal function causes cells to undergo uncontrolled proliferation. Basing on these facts, my initial hypothesis was that SV40 could be considered a “promoting agent” rather than a “transforming agent”. It does not cause directly DNA mutations, but enhancing proliferation, facilitates cells to accumulate DNA mutations caused by other agents. Asbestos is one of these agents and its cooperation with SV40 in causing MM has been already extensively studied *in vitro* and *in vivo*. During the stage in the laboratory of Prof. Carbone, I had the opportunity to continue the studies previously performed in Italy. One of my present projects is aimed at verifying if SV40 can promote full oncogenicity of human mesothelial cells *per se*. At this purpose, we infected with SV40 mesothelial cells obtained from different donors and, after three weeks, we injected them in the peritoneum of immuno-compromised mice. The results revealed that several mice developed MM, indicating that SV40 could be a transforming agent. This led to correct my first

hypothesis on SV40 and new experiments must be performed to understand if mesothelial cell transformation occurred exclusively by SV40 exposure or other concurrent causes, as passages of *in vitro* cultures, may have contributed to this outcome.

Recent data obtained in Gaudino's laboratory allowed us to demonstrate that asbestos and erionite differently cause transformation of human mesothelial cells. Both these minerals are reported to cause DNA damage *in vitro* but, differently to erionite, asbestos kills mesothelial cells [17]. NF-kB and PI3K/Akt signaling play a crucial role in improve resistance to toxic fibers contributing to mesothelial cell transformation. It was found that, after asbestos exposure, there is an inflammatory reaction with a large component of mononuclear phagocytes. Upon differentiation into macrophages, these cells phagocytize asbestos and, as a response, release numerous cytokines and growth factors. Among the cytokines, TNF-α has been linked to MM pathogenesis for its ability to inhibit asbestos-induced cytotoxicity through NF-kB dependent pathway [28]. The activation of upstream tyrosine kinase receptors, such as Epidermal Growth Factor Receptor (EGFR), Plateled Derived Growth Factor Receptor (PDGFR) and Hepatocyte Growth Factor receptor Met, is instead associated to the anti-apoptotic effect of the PI3K/Akt pathway [16, 29, 30]. In the other hand, we demonstrated that erionite does not kill mesothelial cells *in vitro* and induces more DNA damage than asbestos. These results could explain the stronger carcinogenic potential of erionite. Presently, in Carbone's lab we aim at confirming these results *in vivo*, by injecting crocidolite asbestos and erionite in the peritoneum of BALB/c mice. After 8 months, the majority of crocidolite injected mice developed MM and died. Conversely, erionite injected mice did not still developed MM. These results indicate that a longer latency time could be needed for erionite to cause MM. We expect that erionite injected mice develop MM and, for this reason, we will monitor them for tumor formation until to 24 months. In the same experiments, we are also comparing erionite minerals from different Cappadocian villages to verify if these samples have similar biological

effects. This result would confirm the role of genetic predisposition in MM epidemic in Turkey.

I conducted different studies regarding MM therapy together with Prof. Gaudino. The *in vitro* studies on the association of imatinib mesylate with chemotherapy helped me to understand the different behavior of MM cells to different chemotherapy drugs. Furthermore, by performing *in vivo* studies on the mouse model, we defined the side effects that different chemotherapy drugs can cause on different tissues. Our mouse model is innovative, because is the only MM animal model that allows following the fate of cancer cells in living animals by IVIS imaging. Using this model, we can measure tumor dimension changes over time in consequence of a therapeutic treatment and also the related side effects. However, this model is a xenogeneic model in SCID mouse and is limited by the lack of animal immune response. The contribution of immune system in cancer therapy is very important and, at this purpose, we are now in the final phase to establish a syngeneic mouse MM model. We injected mouse MM cells isolated from tumors obtained injecting asbestos in the peritoneum of BALB/c mice. Previously, to allow detection of these cells by IVIS imaging, we infected them with a lentiviral vector carrying the *luciferase* gene. This syngeneic model is now available with two MM cell lines with different biological and molecular features. In the near future we will use it for therapy studies using a new antibody against TGF-β or Onconase®, a new RNAse for treatment of MM.

During my PhD program I have accumulated a sufficient amount of experience on MM therapy and, in conclusion, I would like to express my personal idea on this topic. MM patients are usually treated with standard drugs regardless the chemo-sensitivity of tumor cells. Analyzing the response rates achieved in phase II and III clinical trials, most single chemotherapy agents exhibited very low intrinsic activity. Furthermore, responses rates are generally greater for combination than single-agent regimens [31]. My personal opinion is that higher response rates, obtained using a combination of two drugs, are resulting principally from the higher probability that a patient can respond to one of these

two drugs than a single treatment. Specifically, I assume that every patient with MM shows different chemoresistance patterns derived from the molecular characteristics of the tumor cells. In our experiments, MM cells obtained from different patients displayed different sensibilities to different drugs *in vitro* [25]. In particular, by using simple viability assays we tested three different cell lines to assess drug lethal concentrations (LC_{50}) of gemcitabine and pemetrexed. All tested cell lines show very different LC_{50} for the two drugs. For example, MTT assays performed on REN cells displayed an LC_{50} for gemcitabine of 4.0×10^{-8} and for pemetrexed of 5.0×10^{-5}. Moreover, these MM cells that were found susceptible to gemcitabine but resistant to pemetrexed *in vitro,* revealed the same chemo-susceptible phenotype *in vivo* after injection in SCID mice [26]. On the basis of these results, I propose that it may be possible to preselect patients by viability assays to evaluate the drug resistances directly on living cancer cells obtained from tumor biopsy. Since there are no clinical or biological predictive biomarkers that can reliably identify chemoresistant groups, such simple *in vitro* analysis, would allow the selection of the drug most effective for a given patient. Moreover, during follow-up, repeated biopsy of the progressing tumor could help to identify chemosensitivity changes that allow the tumor to escape treatment. Analysis of tumor biopsies by molecular biology techniques before, during and after treatment could also assist to identify the relevant molecular target of the study drug and its modulation by the treatment administered. Development of accurate and fast procedures to isolate in culture tumor specimens, might allow this personalized treatment in the near future, and help patients who are unlikely to respond to standard therapy.

REFERENCES

1. Margery J, Ruffie P. [Malignant pleural mesothelioma: interrogations and hopes concerning the expected epidemic]. Rev Pneumol Clin 2007 Dec;63(6):354-64.

2. Carbone M, Kratzke RA, Testa JR. The pathogenesis of mesothelioma. Semin Oncol 2002 Feb;29(1):2-17.

3. Upadhyay D, Kamp DW. Asbestos-induced pulmonary toxicity: role of DNA damage and apoptosis. Exp Biol Med (Maywood) 2003 Jun;228(6):650-9.

4. Mossman BT, Bignon J, Corn M, et al. Asbestos: scientific developments and implications for public policy. Science 1990 Jan 19;247(4940):294-301.

5. Dogan AU, Baris YI, Dogan M, et al. Genetic predisposition to fiber carcinogenesis causes a mesothelioma epidemic in Turkey. Cancer Res 2006 May 15;66(10):5063-8.

6. Cicala C, Pompetti F, Carbone M. SV40 induces mesotheliomas in hamsters. Am J Pathol 1993 May;142(5):1524-33.

7. Gazdar AF, Butel JS, Carbone M. SV40 and human tumours: myth, association or causality? Nat Rev Cancer 2002 Dec;2(12):957-64.

8. Jasani B, Cristaudo A, Emri SA, et al. Association of SV40 with human tumours. Semin Cancer Biol 2001 Feb;11(1):49-61.

9. Butel JS, Lednicky JA. Cell and molecular biology of simian virus 40: implications for human infections and disease. J Natl Cancer Inst 1999 Jan 20;91(2):119-34.

10. Dang-Tan T, Mahmud SM, Puntoni R, Franco EL. Polio vaccines, Simian Virus 40, and human cancer: the epidemiologic evidence for a causal association. Oncogene 2004 Aug 23;23(38):6535-40.

11. Cutrone R, Lednicky J, Dunn G, et al. Some oral poliovirus vaccines were contaminated with infectious SV40 after 1961. Cancer Res 2005 Nov 15;65(22):10273-9.

12. Artvinli M, Baris YI. Malignant mesotheliomas in a small village in the Anatolian region of Turkey: an epidemiologic study. J Natl Cancer Inst 1979 Jul;63(1):17-22.

13. Baris YI, Sahin AA, Ozesmi M, et al. An outbreak of pleural mesothelioma and chronic fibrosing pleurisy in the village of Karain/Urgup in Anatolia. Thorax 1978 Apr;33(2):181-92.

14. Carthew P, Hill RJ, Edwards RE, Lee PN. Intrapleural administration of fibres induces mesothelioma in rats in the same relative order of hazard as occurs in man after exposure. Hum Exp Toxicol 1992 Nov;11(6):530-4.

15. Roushdy-Hammady I, Siegel J, Emri S, et al. Genetic-susceptibility factor and malignant mesothelioma in the Cappadocian region of Turkey. Lancet 2001 Feb 10;357(9254):444-5.

16. Cacciotti P, Libener R, Betta P, et al. SV40 replication in human mesothelial cells induces HGF/Met receptor activation: a model for viral-related carcinogenesis of human malignant mesothelioma. Proc Natl Acad Sci U S A 2001 Oct 9;98(21):12032-7.

17. Bertino P, Marconi A, Palumbo L, et al. Erionite and asbestos differently cause transformation of human mesothelial cells. Int J Cancer 2007 Jul 1;121(1):12-20.

18. Abou-Jawde R, Choueiri T, Alemany C, Mekhail T. An overview of targeted treatments in cancer. Clin Ther 2003 Aug;25(8):2121-37.

19. George D. Platelet-derived growth factor receptors: a therapeutic target in solid tumors. Semin Oncol 2001 Oct;28(5 Suppl 17):27-33.

20. Taylor JR, Brownlow N, Domin J, Dibb NJ. FMS receptor for M-CSF (CSF-1) is sensitive to the kinase inhibitor imatinib and mutation of Asp-802 to Val confers resistance. Oncogene 2006 Jan 5;25(1):147-51.

21. Kindler HL, van Meerbeeck JP. The role of gemcitabine in the treatment of malignant mesothelioma. Semin Oncol 2002 Feb;29(1):70-6.

22. Green MR. The evolving role of gemcitabine and pemetrexed (Alimta) in the management of patients with malignant mesothelioma. Clin Lung Cancer 2002 Mar;3 Suppl 1:S26-9.

23. Marangolo M, Vertogen B. Pemetrexed and malignant pleural mesothelioma. Ann Oncol 2006 May;17 Suppl 5:v103-5.

24. Tallarida RJ, Raffa RB. Testing for synergism over a range of fixed ratio drug combinations: replacing the isobologram. Life Sci 1996;58(2):PL 23-8.

25. Bertino P, Porta C, Barbone D, et al. Preliminary data suggestive of a novel translational approach to mesothelioma treatment: imatinib mesylate with gemcitabine or pemetrexed. Thorax 2007 Aug;62(8):690-5.
26. Bertino P, Piccardi F, Porta C, et al. Imatinib mesylate enhances therapeutic effects of gemcitabine in human malignant mesothelioma xenografts. Clin Cancer Res 2008 Jan 15;14(2):541-8.
27. Sablina AA, Hahn WC. SV40 small T antigen and PP2A phosphatase in cell transformation. Cancer Metastasis Rev 2008 Jun;27(2):137-46.
28. Yang H, Bocchetta M, Kroczynska B, et al. TNF-alpha inhibits asbestos-induced cytotoxicity via a NF-kappaB-dependent pathway, a possible mechanism for asbestos-induced oncogenesis. Proc Natl Acad Sci U S A 2006 Jul 5;103(27):10397-402.
29. Zang Y, Hou F, Zhang X. [Effects of epidermal growth factor (EGF) on proliferation of human peritoneal mesothelial cells]. Zhonghua Nei Ke Za Zhi 1996 Feb;35(2):92-4.
30. Langerak AW, De Laat PA, Van Der Linden-Van Beurden CA, et al. Expression of platelet-derived growth factor (PDGF) and PDGF receptors in human malignant mesothelioma in vitro and in vivo. J Pathol 1996 Feb;178(2):151-60.
31. Fennell DA, Gaudino G, O'Byrne KJ, et al. Advances in the systemic therapy of malignant pleural mesothelioma. Nat Clin Pract Oncol 2008 Mar;5(3):136-47.